On the relationship between the mean flow and subgrid stresses in large eddy simulation of turbulent shear flows

L. Shao, S. Sarkar, and C. Pantano

Citation: Physics of Fluids (1994-present) **11**, 1229 (1999); doi: 10.1063/1.869895
View online: http://dx.doi.org/10.1063/1.869895
View Table of Contents: http://scitation.aip.org/content/aip/journal/pof2/11/5?ver=pdfcov
Published by the AIP Publishing

On the relationship between the mean flow and subgrid stresses in large eddy simulation of turbulent shear flows

L. Shao[a)]
Laboratoire de Mécanique des Fluides et d'Acoustique, Ecole Centrale de Lyon, 69130, Ecully, BP 163, France

S. Sarkar[b)] and C. Pantano[c)]
Department of Applied Mechanics and Engineering Sciences, University of California at San Diego, La Jolla, California 92093-0411

(Received 19 May 1998; accepted 27 January 1999)

The present study sheds light on the subgrid modeling problem encountered in the large eddy simulation (LES) of practical flows, where the turbulence is both inhomogeneous and anisotropic due to mean flow gradients. The subgrid scale stress (SGS) tensor, the quantity that is key to the success of LES, is studied here in such flows using both analysis and direct numerical simulation (DNS). It is shown that the SGS tensor, for the case of inhomogeneous flow, where the filtering operation is necessarily performed in physical space, contains two components: a rapid part that depends explicitly on the mean velocity gradient and a slow part that does not. The characterization, rapid and slow, is adopted by analogy to that used in the modeling of the pressure–strain in the Reynolds-averaged Navier–Stokes equations. In the absence of mean flow gradients, the slow part is the only nonzero component and has been the subject of much theoretical study. However, the rapid part can be important in the inhomogeneous flows that are often encountered in practice. An analytical estimate of the relative magnitude of the rapid and slow components is derived and the distinct role of each component in the energy transfer between the resolved grid scales and the unresolved subgrid scales is identified. Results that quantify this new decomposition are obtained from DNS data of a turbulent mixing layer. The rapid part is shown to play an important role when the turbulence is in a nonequilibrium state with turbulence production much larger than dissipation *or* when the filter size is not very small compared to the characteristic integral scale of the turbulence, as in the case of practical LES applications. More importantly, the SGS is observed to be highly anisotropic due to the close connection of the rapid part with the mean shear. The Smagorinsky eddy viscosity and the scale-similarity models are tested by performing *a priori* tests with data from DNS of the mixing layer. It is found that the scale-similarity model correctly represents the anisotropic energy transfer between grid and subgrid scales that is associated with the rapid part, while the eddy viscosity model captures the dissipation associated with the slow part. This may be a physical reason for the recent successes of the mixed model (Smagorinsky plus scale similarity) reported in the literature. © *1999 American Institute of Physics.*
[S1070-6631(99)02205-9]

I. INTRODUCTION

The large eddy simulation (LES) technique has been developed over the past 30 years with the aim of simulating high-Reynolds number turbulent flow. The LES approach involves the simulation of the governing equations for the ''large'' (grid-scale) eddies with models assumed for the ''small'' (subgrid-scale) eddies. Although LES requires a solution of the three-dimensional, unsteady Navier–Stokes equations, as does DNS (direct numerical simulation), the grids are much coarser than those of DNS because the small scales are not resolved. The smaller computational effort permits LES for high-Reynolds number situations, where DNS would be impossible. LES is still more computationally intensive than applications of classical Reynolds-averaged models. The attractiveness of the LES method lies in the expectation of being able to successfully obtain the statistics of interest with SGS modeling that is both simpler and more universal than Reynolds-averaged modeling. Numerous simple turbulent flows, for example, isotropic turbulence, channel flow, and pipe flow have been simulated with success. The ultimate goal of LES in engineering applications is to predict complex, three-dimensional, high-Reynolds number turbulent flows, for example, around an aircraft or in an engine. However, the development of a reliable LES methodology and accurate subgrid-scale models present significant challenges, even for simpler flows, such as those around bluff bodies. These challenges have prompted vigorous re-

[a)]Electronic mail: shao@athena.mecaflu.ec-lyon.fr
[b)]Electronic mail: sarkar@ames.ucsd.edu
[c)]Electronic mail: cpantano@ames.ucsd.edu

search in both theory and application of LES, as discussed in recent reviews by Lesieur and Métais,[1] Moin,[2] and Piomelli and Chasnov.[3]

The large scales are obtained by introducing a spatial filter that operates on the flow field (see Leonard[4]) to remove the unresolvable, small scales of turbulence. Simple flows such as homogeneous turbulence can be simulated with periodic boundary conditions and the Fourier transform in such flows permits the use of the spectral cutoff filter. This spectral cutoff filter is an ideal filter because it defines the grid-scale (GS) and the subgrid-scale (SGS) components exactly; that is, the GS and the SGS are clearly separated in length scale. On the other hand, in most practical computations, the turbulence is not homogeneous and, consequently, filters in the physical domain are required. Popular filters are the top hat filter and the Gaussian filter. However, such filtering results in SGS motion, which involves a dominant contribution of the small length scales as well as a smaller contribution of the large scales; consequently, the unambiguous separation of scales is not achieved. Thus, the subgrid model may necessarily have to depend on the type of the filter. The dependence of the subgrid model on the filter has been studied by Piomelli, Moin, and Ferziger.[5] They showed that the subgrid model used in a LES must depend on the filter, for example, the scale-similarity model is not suitable for the spectral cutoff filter. Recent developments in SGS modeling such as the dynamic procedure introduced by Germano, Piomelli, Moin, and Cabot[6] and the scale-similarity model of Bardina, Ferziger, and Reynolds[7] later refined by Liu, Meneveau, and Katz[8] and Salvetti and Banerjee,[9] require explicit filtering. With the necessity of physical-space filtering in inhomogeneous flows as well as the success and promise of the recent models that require explicit filtering, it is clear that the role of filtering in SGS modeling deserves attention.

The two primary effects that require modeling in LES of turbulent shear flows are the following: first, the SGS shear stress whose gradient directly impacts the mean flow, and second, the net energy transfer between the large and small scales, which includes both the dominant dissipative effect associated with the forward transfer from large to small eddies and the backward energy transfer from small to large scales. The backward transfer is often small compared to the forward transfer, except near solid walls. Using the assumption of isotropy of the small scales by analogy to molecular diffusion, one can introduce an ''eddy viscosity'' to take into account the forward-transfer mechanism and can relate the unknown SGS stress to the resolved GS motion. The well-known Smagorinsky model[10] is the most popular ''eddy viscosity'' model for the unresolved small scales. When used in its original form or its recent variants (like the dynamic model), or when used in combination with other models such as the scale-similarity model of Bardina *et al.*,[7] the Smagorinsky model is probably the most popular choice in LES applications.

For the most part, the theoretical background for modeling the effect of small scales in a LES application has remained within the framework of homogeneous turbulence. Various theories of SGS modeling have been developed by Kraichnan,[11] Leslie and Quarini,[12] Leith,[13] Chollet and Lesieur,[14] Bertoglio and Mathieu,[15] etc. In most cases the Kolomogorov cascade theory is implicitly used to represent the SGS transfer. However, it is unlikely that, for routine engineering applications, computational resources will allow the fine resolution required for such an approximation of isotropic, homogenous small-scale turbulence to be acceptable. Furthermore, small scales are anisotropic and inhomogeneous in *nonequilibrium* turbulence with turbulence production much larger than dissipation that occurs, for example, in rapid distortions or in the presence of suddenly imposed body forces. For the more important applications where the turbulence is inhomogeneous, fundamental studies are rare. Schumann[16] introduced a two-part eddy viscosity model: a *homogeneous* part that accounts for the ''locally isotropic'' part of the SGS stress and an *inhomogeneous* part to represent the anisotropy associated with the use of a large filter size. The inhomogeneous part is directly related to the Reynolds-averaged strain rate in the spirit of a classical eddy viscosity closure. This model has also been used with some success by Sullivan *et al.*[17] for LES of the planetary boundary layer. The SGS energy transfer mechanism in case of wall-bounded turbulent flows has been investigated in detail by Domaradzki *et al.*[18] Recently, O'Neil and Meneveau[19] performed an experimental study of the SGS stresses in an inhomogeneous turbulent wake. They found that the large coherent structures in the wake strongly affect the SGS stress. Thus, the local inhomogeneity of the flow and the associated coherent structures influences the SGS stress in a wake and may require modeling.

In the present study we explore the implications of physical-space filtering in SGS modeling of inhomogeneous flows in both nonequilibrium and equilibrium turbulence. In order to develop an understanding in the context of mean statistics, which are of the greatest interest in engineering predictions, we use the Reynolds decomposition to split the flow into a mean and a centered fluctuating flow. The fluctuation represents the turbulence. In the present paper we explore the various consequences of LES of inhomogeneous flow on the filtering approach, on the energetics of the interaction between the grid scale and the subgrid scale, on the anisotropy of this interaction, and, finally, on the fidelity of existing SGS models. Section II is a theoretical analysis of the effect of the mean velocity gradient on the form of the SGS stress tensor as well as its influence on the mean flow/resolved turbulence/subgrid turbulence interactions. An explicit effect of the mean velocity gradient on the SGS stress tensor resulting from physical-space filtering is found. By analogy with the decomposition of the pressure–strain correlation into rapid and slow parts (see Lumley[20]), we define a rapid SGS stress tensor that depends explicitly on the mean velocity gradient and a slow SGS stress tensor that depends only on the fluctuating velocity. The rapid component reacts instantaneously to a change in the mean flow; the slow component does not. The role of these components is analyzed by considering their relative magnitude and their impact on the energy exchange between the mean flow, large-scale turbulence, and small-scale turbulence. In Sec. III, DNS data of the temporally evolving turbulent mixing layer of Pantano and Sarkar[21] is used to perform an *a priori* comparison of the

various SGS stress tensors at a tensor level (component by component) and at a scalar level, that is, in the SGS energy exchange. The applicability of various SGS models to represent the intrinsically different effects of the rapid and slow parts of the SGS tensor is examined in Sec. IV.

II. ANALYSIS OF FILTERING IN INHOMOGENEOUS FLOWS

Central to the spirit of LES, a filter is introduced to separate the large scales from the small scales of motion. Let $f^<$, equivalently $\bar{f}$, denote the filtered value of the variable f that nominally represents the large-scale variation. The filter is usually defined (Leonard[4]) as follows:

$$f^<(x)=\int_\Omega f(x')g(x-x')dx, \qquad \int_\Omega g(x)dx=1. \tag{1}$$

In Eq. (1), g is the kernel function of the filter and the integral is over the domain Ω of the function f.

In LES, only the filtered velocity $u_i^<$, also called the grid-scale (GS) velocity, is explicitly computed; thus, from Eq. (1),

$$u_i^<(x)=\int_\Omega u_i(x')g(x-x')dx'. \tag{2a}$$

Note that $u_i^{<<}\neq u_i^<$ except when filtering is performed with a spectral cutoff filter, which is an exact low-pass filter in wave number space. The unresolved, subgrid-scale (SGS) velocity, denoted by $u_i^>$, is given by

$$u_i^>=u_i-u_i^<. \tag{2b}$$

This separation of the scales depends strongly on the type of the filter that is used. In homogeneous turbulence, filtering can be done in spectral space with the spectral cutoff filter. Since such spectral-space filtering clearly achieves a global separation of scales, it has been popular in the analysis and development of SGS models as well as in the application of LES to flows with homogeneous directions.

In typical applications, flows are inhomogeneous in one or more directions; spectral-space filtering is not possible in such directions. Furthermore, the SGS modeling approach may restrict the use of the spectral cutoff filter; the scale-similarity model is one such example, as shown by Liu, Meneveau, and Katz.[8] Thus, physical-space filters such as the Gaussian filter and the top hat filter have become popular in LES applications.

We now discuss the consequences of physical-space filtering.

A. The ensemble-averaged velocity

Ensemble averaging allows the definition of a mean velocity $\langle u_i\rangle$ and a centered fluctuating velocity u_i', and the following Reynolds decomposition ensues:

$$u_i=\langle u_i\rangle+u_i'. \tag{3}$$

The application of the filtering operation to the mean and fluctuating velocity, respectively, gives

$$\langle u_i\rangle=\langle u_i^<\rangle+\langle u_i^>\rangle, \tag{4}$$

$$u_i'=u_i'^<+u_i'^>. \tag{5}$$

Equation (5) implies that both the GS and SGS velocities contribute to the ensemble-averaged mean. The presence of a nonzero value of the mean SGS velocity, $\langle u_i^>\rangle$, is not desirable because it leads to a breakdown in the separation of scales between filtered and unfiltered quantities. Of course, filtering in spectral space with the cutoff filter would ensure zero mean of the SGS velocity; however, inhomogeneity of the turbulence prevents the use of the cutoff filter.

We now compare the effects of physical-space filtering in a direction with constant mean velocity with that in a direction with nonuniform mean velocity. From the definition, Eq. (1), if the mean velocity is a constant, $\langle u_i^>\rangle=0$, since the filtered value of a constant is just the constant itself. Thus, for this situation, the subgrid component contributes only to the turbulent fluctuation and filtering does not violate the separation of scales. The top hat filter when applied to a constant-gradient mean velocity also results in $\langle u_i^>\rangle=0$.

On the other hand, the application of the top hat filter to an inhomogeneous direction (with a nonuniform mean velocity gradient) leads to a nonzero mean component in the SGS velocity: $\langle u_i^>\rangle\neq 0$. Thus, an important property of filtering in the inhomogeneous direction is the introduction of a *nonzero mean* SGS velocity. Next we will examine the effect of physical-space filtering on the SGS stress tensor.

B. Subgrid stress tensors

Before discussing the effect of physical-space filtering on the SGS stress tensor, we recall the following definitions.

The GS (grid-scale) stress tensor is given by

$$R_{ij}^<=u_i^<u_j^<, \tag{6}$$

while the primitive SGS (subgrid-scale) stress tensor is defined by

$$T_{ij}=u_iu_j-u_i^<u_j^<. \tag{7}$$

The adjective ''primitive'' is used because this subgrid-scale stress tensor is not identical to the one that appears in the LES equations, the commonly called SGS stress tensor, τ_{ij}, which is defined by

$$\tau_{ij}=(u_iu_j)^<-u_i^<u_j^<. \tag{8}$$

The relation between these two tensors is a Germano identity at the no-filter level (zero level) and one-filter level (f level):

$$\tau_{ij}=T_{ij}^<+l_{ij}, \tag{9}$$

in which l_{ij} is the Leonard term:

$$l_{ij}=(u_i^<u_j^<)^<-u_i^<u_j^<. \tag{10a}$$

If the filter used is of the spectral cutoff type, the Leonard term is a numerical error like the aliasing error encountered in LES with the pseudospectral method and can be removed easily.

Another SGS tensor is the ''resolved'' part of the SGS tensor, L_{ij}, given by

$$L_{ij}=(u_i^{<}u_j^{<})^{<}-u_i^{\ll}u_j^{\ll}. \tag{10b}$$

The importance of L_{ij} stems from its use in the scale-similarity model for τ_{ij}.

Note that usually only the deviatoric part of the SGS tensor, $\tau_{ij}-\tau_{kk}/3$, is considered. The isotropic part, $\tau_{kk}/3$, is absorbed into a generalized pressure.

C. A new split of the SGS tensor into rapid and slow components

The SGS tensor τ_{ij} represents, in the spirit of LES, the effect of the interaction between the resolved ''large scales,'' $u_i^{<}$, and the unresolved ''small scales,'' $u_i^{>}$. To understand the effect of mean-flow gradients on the subgrid-scale stress τ_{ij}, we use the Reynolds decomposition of the velocity into mean and fluctuating components.

The SGS tensor τ_{ij} obtained after using Eq. (3) for the velocity can be split into two parts: a *rapid part* that explicitly depends on the mean flow and a remaining *slow part*. The term ''rapid'' is used by analogy to the terminology introduced by Lumley[20] in the context of Reynolds-averaged modeling, where the component of the pressure–strain term that explicitly depends on the mean velocity gradient is referred to as the rapid part and the remainder as the slow part. Thus, τ_{ij} is split as follows:

$$\tau_{ij}=\tau_{ij}^{\mathrm{Rapid}}+\tau_{ij}^{\mathrm{Slow}}, \tag{11}$$

where

$$\tau_{ij}^{\mathrm{Slow}}=(u_i'u_j')^{<}-u_i'^{<}u_j'^{<}, \tag{12a}$$

$$\tau_{ij}^{\mathrm{Rapid}}=(\langle u_i\rangle\langle u_j\rangle)^{<}-\langle u_i^{<}\rangle\langle u_j^{<}\rangle+(u_i'\langle u_j\rangle)^{<}-u_i'^{<}\langle u_j^{<}\rangle+(u_j'\langle u_i\rangle)^{<}-u_j'^{<}\langle u_i^{<}\rangle. \tag{12b}$$

The *slow* SGS tensor $\tau_{ij}^{\mathrm{Slow}}$ is always present in LES, irrespective of the presence or absence of a mean flow, and its effect and modeling has been discussed (for example, Leslie and Quarini,[12] Kraichnan,[11] Chollet and Lesieur,[14] and Bertoglio and Mathieu,[16] among others), in the case of isotropic or homogeneous turbulence. The *rapid* SGS tensor $\tau_{ij}^{\mathrm{Rapid}}$ arises only if the filtering is done in a direction where $\langle u_i\rangle$ is *not* constant. It should be noted that, distinct from this explicit contribution of the mean-flow gradient to the subgrid-scale stress through $\tau_{ij}^{\mathrm{Rapid}}$, there would be an implicit effect of the mean flow on $\tau_{ij}^{\mathrm{Slow}}$, which could require additional modifications to models based on homogeneous isotropic turbulence when applied to inhomogeneous flows.

The nature of $\tau_{ij}^{\mathrm{Rapid}}$ is different from that of $\tau_{ij}^{\mathrm{Slow}}$. For example, even when the flow is laminar, the first line in Eq. (12b) persists in the inhomogeneous direction while the two others vanish. Furthermore, as will be shown in the next section, the magnitude of $\tau_{ij}^{\mathrm{Rapid}}$ depends on the gradient of the mean velocity. Therefore, the time scale of its response to mean flow changes is short and, as will be shown, its magnitude with respect to the slow part is larger for rapid distortion flows. If the ensemble-averaged field is subtracted before performing filtering, the presence of the rapid term can be avoided. Although possible in *a priori* tests of SGS models, this is not a solution in the application of LES to an inhomogeneous flow, because the mean flow is not known in advance. The rapid term is a consequence of filtering in the inhomogeneous direction. In principle, filtering could be performed only in the homogeneous directions, if they are present, in order to avoid the rapid term. In practice, filtering is required in all directions, regardless of flow inhomogeneity, because resolution down to the smallest Kolmogorov scale that is required in the direction without filtering would excessively increase the size of the computational grid.

D. Relative size of rapid and slow terms

An estimate, based on a second-order Taylor series expansion, of the relative size of the slow and rapid terms is presented below for the top hat filter. It should be noted that the estimate is approximate because a low-order Taylor series expansion can have large inaccuracy in estimating local variations in the velocity fluctuation. DNS will be used later for a more precise, quantitative comparison.

Using the Taylor series expansion of the filter introduced by Clark, Ferziger, and Reynolds[22] in their derivation of the gradient-type subgrid model, Eq. (1) can be approximated by

$$f^{<}(x)=f(x)+\frac{\Delta_k^2}{24}\partial_k^2 f(x)+O(\Delta^4), \tag{13a}$$

which leads to

$$f^{>}(x)=-\frac{\Delta_k^2}{24}\partial_k^2 f(x)+O(\Delta^4). \tag{13b}$$

Note that the first derivative drops out of the rhs of Eq. (13a) since a symmetric filter is assumed. Here, Δ_k is the spatial width of a symmetric filter in the kth direction and ∂_k^2 is the second-order partial derivative in the kth direction. Equation (13) is valid for both Gaussian and top hat filters.

The mean subgrid variable $\langle f^{>}\rangle$ is then

$$\langle f^{>}\rangle(x)=-\frac{\Delta_k^2}{24}\partial_k^2\langle f(x)\rangle+O(\Delta^4). \tag{13c}$$

It should be noticed that the size of this subgrid mean value depends on the second derivative of the mean profile, which is related to the local curvature.

For the two subgrid-scales stresses T_{ij} and τ_{ij}, the corresponding approximate expressions are

$$T_{ij}=-\frac{\Delta_k^2}{24}[\partial_k^2(u_iu_j)-2(\partial_k u_i\partial_k u_j)]+O(\Delta^4), \tag{14a}$$

$$\tau_{ij}=+\frac{\Delta_k^2}{12}\partial_k u_i\partial_k u_j+O(\Delta^4). \tag{14b}$$

The mean value of the rapid SGS stress, $\langle\tau_{ij}^{\mathrm{Rapid}}\rangle$, can be easily evaluated since it contains only the mean velocity gradient. We have

$$\langle\tau_{ij}^{\mathrm{Rapid}}\rangle=\frac{\Delta_k^2}{12}\partial_k\langle u_i\rangle\partial_k\langle u_j\rangle+O(\Delta^4). \tag{15a}$$

Neglecting the $O(\Delta^4)$ term implies that, to leading order, the rapid SGS stress depends on the square of the *mean velocity gradient* and varies as Δ^2. Similarly,

$$\langle \tau_{ij}^{\text{Slow}} \rangle = \frac{\Delta_k^2}{12} \langle \partial_k u_i' \partial_k u_j' \rangle + O(\Delta^4). \tag{15b}$$

The error incurred by neglecting the $O(\Delta^4)$ term in Eq. (15b) is larger than in Eq. (15a); nevertheless, the estimate is appropriate for a sufficiently small filter size.

As an example, consider the DNS test case used in the present study (the temporally evolving mixing layer), $\partial_k \langle u_i \rangle = S$, for $i=1$ and $k=2$, and zero otherwise. The resulting approximation for the mean rapid SGS stress is then

$$\langle \tau_{ij}^{\text{Rapid}} \rangle = \frac{\Delta_2^2}{12} S^2 \delta_{i1} \delta_{j1} + O(\Delta^4), \tag{15c}$$

and, assuming an isotropic filter, for the mean slow SGS stress:

$$\langle \tau_{ij}^{\text{Slow}} \rangle = \frac{\Delta^2}{12} \langle \partial_k u_i' \partial_k u_j' \rangle + O(\Delta^4). \tag{15d}$$

The only important mean rapid SGS stress component is the 11 component, given by

$$\langle \tau_{11}^{\text{Rapid}} \rangle = \frac{\Delta^2}{12} S^2 + O(\Delta^4). \tag{15e}$$

The scaling given by Eq. (15e) is checked later in the results section. From this simple example of the temporally evolving mixing layer, it is clear that the rapid component has an anisotropy that is directly related to the mean-flow gradients.

How large is the rapid term relative to the slow term? When the filter size is small, Eq. (15b) applies, and after using $\langle \partial_k u_i' \partial_k u_j' \rangle = O(\epsilon/\nu)$, it follows that

$$\frac{\langle \tau_{ij}^{\text{Rapid}} \rangle}{\langle \tau_{ij}^{\text{Slow}} \rangle} = O\left(\frac{\nu S^2}{\epsilon} \right) = O\left(\frac{\nu S}{u^2} \frac{P}{\epsilon} \right) = O\left(\frac{1}{\text{Re}_\omega} \right) \left(\frac{U^2}{u^2} \right) \left(\frac{P}{\epsilon} \right). \tag{16a}$$

Here, U denotes the mean velocity difference, u denotes the rms value of the turbulence; the turbulence production has been estimated by $P = O(Su^2)$ and the Reynolds number, $\text{Re}_\omega = U\delta_\omega/\nu$, is defined using the vorticity thickness that is estimated by $\delta_\omega = O(U/S)$. Thus, for equilibrium turbulence with $P/\epsilon = O(1)$, and at a high Reynolds number, the rapid part is small compared to the slow part for a sufficiently small filter size. However, for nonequilibrium turbulence with $P/\epsilon > O(1)$, the rapid part may become comparable to the slow part.

There is another situation where the rapid part may be of importance. In practice, the filter size in LES of complex flows may not be much smaller than the integral length scale. In such a situation a low-order Taylor-series expansion of the velocity fluctuation does not apply, and therefore Eq. (15d) must be replaced by

$$\langle \tau_{ij}^{\text{Slow}} \rangle = O(u^2), \tag{16b}$$

which leads to

$$\frac{\langle \tau_{ij}^{\text{Rapid}} \rangle}{\langle \tau_{ij}^{\text{Slow}} \rangle} = O\left(\frac{S^2 \Delta^2}{u^2} \right) = O\left(\frac{S^2 l^2}{u^2} \right) \left(\frac{\Delta^2}{l^2} \right). \tag{16c}$$

Here l is a characteristic integral scale of the turbulence. Since $Sl/u = O(1)$ in shear-driven turbulence, the rapid part can become comparable to the slow part when the filter size increases, such that $\Delta/l = O(1)$. The magnitude of the rapid component is even larger when the turbulence is in nonequilibrium with $Sl/u > O(1)$.

E. The energy transfer mechanism between grid and subgrid scales

It is important to identify clearly the energy transfer mechanisms between the different scales of motion and ensure that the model for the subgrid-scale tensor τ_{ij} represents these mechanisms. Let us first recall the interaction between mean and fluctuating fields in the context of the Reynolds-averaged approach. The equation for the kinetic energy, $\langle u_i \rangle^2/2$, of the mean motion is

$$\partial_t \frac{\langle u_i \rangle^2}{2} + \langle u_j \rangle \partial_j \left(\frac{\langle u_i \rangle^2}{2} \right) = \langle u_i' u_j' \rangle \langle S_{ij} \rangle - \text{pres term} + \text{visc term}, \tag{17a}$$

while the equation for the turbulent kinetic energy, $\langle u_i'^2 \rangle/2$, is

$$\partial_t \left\langle \frac{u_i'^2}{2} \right\rangle + \langle u_j \rangle \partial_j \left\langle \frac{u_i'^2}{2} \right\rangle + \partial_j \left\langle u_j' \frac{u_i'^2}{2} \right\rangle = -\langle u_i' u_j' \rangle \langle S_{ij} \rangle - \text{pres term} - \text{visc term}. \tag{17b}$$

Here S_{ij} is the rate of strain tensor and s_{ij}' is its fluctuating part. The coupling between mean and fluctuating kinetic energy is by the production term, $-\langle u_i' u_j' \rangle \langle S_{ij} \rangle$, denoted by P. It is usually positive, draining energy from the mean flow into the turbulence. The third term of Eq. (17b), which can be rewritten as $\langle u_i' u_j' s_{ij}' \rangle$, represents the self-interaction between various scales of turbulence.

Now consider the energy transfer mechanisms in LES. We follow the approach of Haertel, Kleiser, Unger, and Friedrich,[23] who consider interactions between the kinetic energy associated with the ensemble-mean grid-scale (GS) velocity, the fluctuating GS velocity and the fluctuating SGS velocity. From the transport equation for the grid-scale velocity,

$$\partial_t u_i^< + \partial_j u_i^< u_j^< = -\partial_j \tau_{ij} - P^</\rho + \nu \partial_{jj} u_i^<, \tag{18}$$

in which $P^<$ is the filtered pressure and does not include the trace $\tau_{kk}/3$, it is straightforward to derive transport equations for the GS mean and fluctuating kinetic energies, $\langle u_i^< \rangle^2/2$ and $\langle u_i'^{<2} \rangle/2$, respectively. The role of the SGS stress in these transport equations for the kinetic energies can be better understood by splitting τ_{ij} into a mean and fluctuating component. Then the primary energy transfer term associated with the SGS stress, $-\langle \tau_{ji} S_{ij}^< \rangle$, also called the SGS dissipation, is split into a mean and fluctuation part:

$$\langle \tau_{ji} S_{ij}^< \rangle = \langle \tau_{ji} \rangle \langle S_{ij}^< \rangle + \langle \tau_{ji}' s_{ij}'^< \rangle. \tag{19}$$

Here, $\langle S_{ij}^{<}\rangle$ and $s_{ij}'^{<}$ are the mean and fluctuating parts of the grid-scale rate of strain tensor, respectively.

The equation for the mean GS kinetic energy is

$$\partial_t \frac{\langle u_i^{<}\rangle^2}{2} + \langle u_j^{<}\rangle \partial_j \left(\frac{\langle u_i^{<}\rangle^2}{2} \right) = \langle u_i^{<\prime} u_j^{<\prime}\rangle \langle S_{ij}^{<}\rangle + \langle \tau_{ij}\rangle \langle S_{ij}^{<}\rangle + \text{turb transp term} + \text{pressure term} + \text{visc term}, \tag{20a}$$

while the equation for the turbulent GS kinetic energy is

$$\partial_t \frac{\langle u_i'^{<2}\rangle}{2} + \langle u_j^{<}\rangle \partial_j \left(\frac{\langle u_i'^{<2}\rangle}{2} \right) = -\langle u_i^{<\prime} u_j^{<\prime}\rangle \langle S_{ij}^{<}\rangle + \langle \tau_{ij}' s_{ij}'^{<}\rangle - \langle u_i^{<\prime} u_j^{<\prime} s_{ij}'^{<}\rangle + \text{turb transp term} + \text{pressure term} + \text{visc term}. \tag{20b}$$

In order to simplify the interpretation of the above equations, we do not consider the last three terms: the turbulent transport, the pressure term, and the viscous term.

In order to better describe the effect of rapid and slow components of the SGS stress in the energy transfer process, we will apply the decomposition into mean and fluctuating components proposed by Haertel *et al.*[23] to both, rapid and slow components. Thus,

$$\tau_{ij}^{\text{Rapid}} = \langle \tau_{ij}^{\text{Rapid}}\rangle + \tau_{ij}'^{\text{Rapid}}$$

and

$$\tau_{ij}^{\text{Slow}} = \langle \tau_{ij}^{\text{Slow}}\rangle + \tau_{ij}'^{\text{Slow}}.$$

From Eq. (12b) it is clear that the mean rapid part is given by

$$\langle \tau_{ij}^{\text{Rapid}}\rangle = (\langle u_i\rangle\langle u_j\rangle)^{<} - \langle u_i^{<}\rangle\langle u_j^{<}\rangle, \tag{21a}$$

while the fluctuating part is

$$\tau_{ij}'^{\text{Rapid}} = (u_i'\langle u_j\rangle)^{<} - u_i'^{<}\langle u_j^{<}\rangle + (u_j'\langle u_i\rangle)^{<} - u_j'^{<}\langle u_i^{<}\rangle. \tag{21b}$$

Similarly, the mean part of the slow SGS stress is

$$\langle \tau_{ij}^{\text{Slow}}\rangle = \langle (u_i'u_j')^{<} - u_i'^{<}u_j'^{<}\rangle,$$

while the fluctuating component is given by

$$\tau_{ij}'^{\text{Slow}} = \tau_{ij}^{\text{Slow}} - \langle \tau_{ij}^{\text{Slow}}\rangle.$$

The first term on the right-hand side of Eqs. (20a) and (20b), which is analogous to the production term P in the Reynolds-averaged equations, (17a) and (17b), transfers energy between the mean and fluctuating parts of the GS kinetic energy. The second term, $\langle \tau_{ij}\rangle\langle S_{ij}^{<}\rangle$, on the right-hand side of Eq. (21a), is an interaction between the mean SGS stress and the mean grid-scale motion; the fluctuating grid-scale motion is not involved. This term can be rewritten as

$$\langle \tau_{ij}\rangle\langle S_{ij}^{<}\rangle = \langle \tau_{ij}^{\text{Rapid}}\rangle\langle S_{ij}^{<}\rangle + \langle \tau_{ij}^{\text{Slow}}\rangle\langle S_{ij}^{<}\rangle, \tag{22a}$$

to isolate the effect of the rapid term. The slow term in Eq. (22a) corresponds to the term identified by Haertel *et al.*[23] as representing the subgrid contribution to the total turbulence production P; the part, $P - \langle \tau_{ij}^{\text{Slow}}\rangle\langle S_{ij}^{<}\rangle$, which is a rewritten form of the first term in Eq. (20b), supplies energy to the grid-scale fluctuations while the remainder, $\langle \tau_{ij}^{\text{Slow}}\rangle\langle S_{ij}^{<}\rangle$, is transferred to the subgrid-scale fluctuations. The third term, $\langle \tau_{ij}' S_{ij}'^{<}\rangle$, in Eq. (20b), which appears only in the fluctuating GS energy equation, represents the nonlinear interaction between the GS and SGS parts of the turbulence (usually, forward cascade; sometimes, backward transfer or backscatter). However, if we rewrite this term as

$$\langle \tau_{ij}' s_{ij}'^{<}\rangle = \langle \tau_{ij}'^{\text{Rapid}} s_{ij}'^{<}\rangle + \langle \tau_{ij}'^{\text{Slow}} s_{ij}'^{<}\rangle, \tag{22b}$$

it is clear that there is a component, the rapid part, which contains both mean [due to the presence of mean velocity in $\tau_{ij}'^{\text{Rapid}}$; see Eq. (21b)] and fluctuating velocities, in addition to the slow component, which involves only the fluctuating velocity. The term $\langle \tau_{ij}'^{\text{Rapid}} s_{ij}'^{<}\rangle$ represents a *direct* coupling between the mean velocity and fluctuating SGS velocity, which influences the fluctuating GS energy. DNS will be used to check whether $\langle \tau_{ij}'^{\text{Rapid}} s_{ij}'^{<}\rangle$ represents forward transfer or backscatter.

III. EVALUATION OF THE RAPID AND SLOW SGS TENSORS IN A TURBULENT MIXING LAYER

Results from the DNS of the temporally evolving, turbulent mixing layer by Pantano and Sarkar[21] are used for clarifying the relative importance of the rapid and slow parts of the SGS tensor. A dataset with low convective Mach number, $M_c = 0.3$, is used so that compressibility effects can be neglected.

A priori tests to evaluate the rapid and slow SGS tensors are performed on a tensor level by comparing the magnitude of the mean and rms values of the different directional components, as well as on a scalar level where their relative contributions to the energy transfer between grid scales and subgrid scales are obtained. The tests are performed with DNS results at an early time before the turbulence is fully developed and at a later time. The *top hat* filter is used. Note that the filter is applied *isotropically* in all directions in the *a priori* test. The influence of the filter size is also investigated. The filter size is set to $\Delta_f/\Delta = 2$ and 4 for the early time dataset and $\Delta_f/\Delta = 2$, 4, 6, and 8 at the later time. Here Δ is the grid spacing (uniform in all directions) in the DNS. The temporally evolving mixing layer is inhomogeneous in a single direction along the transverse y coordinate. Consequently, ensemble-averaged statistics are functions of only the y coordinate and can be obtained by averaging the instantaneous flow over x-z planes.

A. The turbulent mixing layer DNS

The three-dimensional, unsteady Navier Stokes equations were numerically solved by Pantano and Sarkar[21] to investigate a temporally evolving turbulent mixing layer. The initial mean velocity profile is $U(y) = (\Delta U/2)\tanh(-y/2\delta_m)$; where $\Delta U = U_1 - U_2$ is the velocity difference between upper and lower streams, and δ_m is the momentum thickness. The initial fluctuations are broadband with an isotropic turbulence spectrum in the horizontal directions, and turbulent kinetic energy that varies in the transverse y direc-

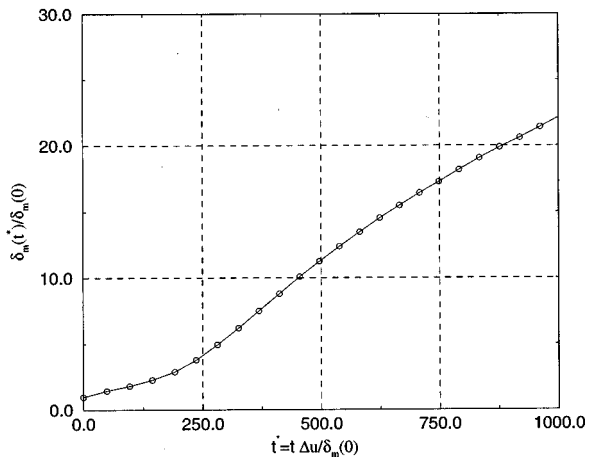

FIG. 1. Evolution of the momentum thickness.

tion as $k/\Delta U^2 \propto \exp(-y^2/2\delta_m^2)$. A low-Mach number case with convective Mach number, $M_C=0.3$, from the DNS is considered here. It is known from experimental data that the shear layer behavior at $M_C=0.3$ deviates little from the incompressible case and, therefore, the $M_C=0.3$ dataset can be considered as effectively incompressible. The initial Reynolds number based on the initial vorticity thickness is $\mathrm{Re}_\omega = \Delta U \delta_{\omega,0}/\nu = 160$. A fourth-order compact finite difference approximation with a fourth-order Runge–Kutta low storage method for the time advancement is used for the numerical solution. A uniform $128\times128\times128$ grid is used.

A summary of pertinent DNS results is provided here. The evolution of the momentum thickness, δ_m, is shown in Fig. 1. After an initial transient, the shear layer evolves in time with a linear growth rate as observed in numerous physical experiments. In the laboratory, the mixing layer grows in the streamwise x direction with the following growth rate law (it is customary to use the vorticity thickness, δ_ω) applicable to the self-similar regime,

$$d\delta_\omega/dx = C_\delta (U_1-U_2)/(U_1+U_2),$$

with a consensus of experimental data giving $C_\delta=0.16$. Assuming a convection velocity of $(U_1+U_2)/2$, the temporal growth rate becomes

$$d\delta_\omega/dt = 0.08\Delta U.$$

The observed growth rate in our DNS is $d\delta_\omega/dt = 0.07\Delta U$, which is in good agreement with the above experimental result. Figures 2(a) and 2(b) show profiles of the turbulence intensities at a late time in the DNS which are seen to be in good agreement with the experimental data of Bell and Mehta.[24]

B. Magnitude of slow and rapid SGS tensor

The total, slow, and rapid components of the SGS tensor are computed as follows. First, the total SGS tensor τ_{ij} is obtained by processing the whole velocity field. Second, the slow part, $\tau_{ij}^{\mathrm{Slow}}$, is computed by processing the centered fluctuating velocity obtained by subtracting the mean, plane-

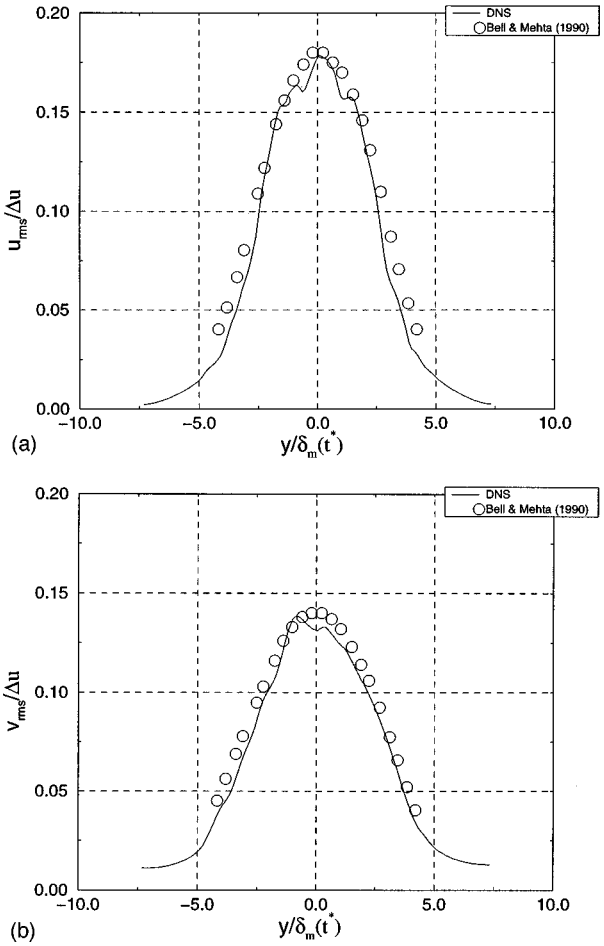

FIG. 2. (a) Profiles of the streamwise turbulence intensity at time step =2500, $t^*=1089$. Symbols denote experimental data from Bell and Mehta (Ref. 24). (b) Profiles of the transverse turbulence intensity at time step =2500, $t^*=1089$. Symbols denote experimental data from Bell and Mehta (Ref. 24).

averaged velocity, $\langle U\rangle(y)$, from the total velocity field. Finally, the difference between the total and the slow SGS stresses gives the rapid SGS stress, $\tau_{ij}^{\mathrm{Rapid}}$. The *a priori* tests are carried out at time $t^*=236$ and $t^*=1089$, corresponding to an early and later stage of the mixing layer, respectively. Here, the normalized value $t^*=\Delta U\, t/\delta_{m,0}$ is used for the time variable. The Reynolds numbers based on a streamwise micro-Taylor scale and rms velocity are 108 at the early stage and 142 at the late stage. Different wave number positions corresponding to different filter sizes used are indicated in Fig. 3(a) (for early stage) and Fig. 3(b) (for later stage) that show centerline, one-dimensional spectra, $Eu_i(k_z,t^*)$, for each velocity component.

At the early time, coherent spanwise rollers and braids are clearly present, as shown in Fig. 4 (left picture), which could influence the mean/grid-scale/subgrid-scale interactions, while at the later time, these coherent structures are not as evident (see Fig. 4, right picture) and there is significant, small-scale, three-dimensional turbulence.

Normalized profiles are obtained by nondimensionalization with the centerline value of appropriate DNS data, at the same time step. The subgrid stresses are normalized with

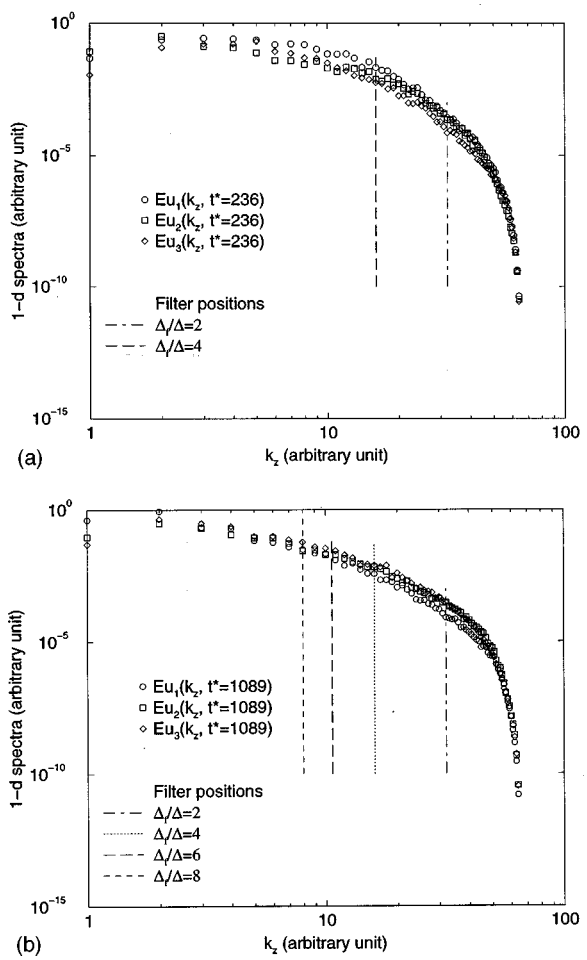

FIG. 3. (a) One-dimensional spanwise spectrum, $Eu_i(k_z,t^*)$, for $i=1$, 3, at time step=500, $t^*=236$. (b) One-dimensional spanwise spectrum, $Eu_i(k_z,t^*)$, for $i=1$, 3, at time step=2500, $t^*=1089$.

twice the turbulent kinetic energy. The mean subgrid energy production (or dissipation) by the mean flow as well as the fluctuating subgrid energy transfer are normalized with the Reynolds-averaged turbulent dissipation ϵ, and the SGS shear stress with the Reynolds-averaged turbulent shear stress.

1. Tensor level

In order to compare the magnitude of the slow and the rapid tensor components, we use ensemble averaging to get the mean and fluctuating components,

$$\tau_{ij}=\langle\tau_{ij}\rangle+\tau'_{ij}.$$

In the present temporally evolving mixing layer, since the mean flow varies only in the y (equivalently x_2) direction, it is clear from the approximate expression of the rapid SGS stress, $\langle\tau_{ij}^{\mathrm{Rapid}}\rangle$, given by Eq. (15c), that the dominant part of this tensor is the 11 component. Therefore, when discussing the rapid SGS stress, attention is focused on the behavior of the $\langle\tau_{11}^{\mathrm{Rapid}}\rangle$ component. A comparison with the slow SGS stress is done with the corresponding 11 component, $\langle\tau_{11}^{\mathrm{Slow}}\rangle$. In addition, the anisotropy of these two tensors is also discussed.

a. Mean SGS stress magnitude and its anisotropy. Figures 5(a)–(b) show the behavior of the 11 component of the mean rapid and the mean slow SGS tensors, $\langle\tau_{11}^{\mathrm{Rapid}}\rangle$ and $\langle\tau_{11}^{\mathrm{Slow}}\rangle$, for the filter size varying from two to four times the grid size, at the early stage of the development of the mixing layer, $t^*=236$. Both increase as the filter size becomes larger. Compared to the slow part, $\langle\tau_{11}^{\mathrm{Rapid}}\rangle$ is approximately three times larger. This is expected at the early stage: first, the turbulence is still evolving, the ratio $P/\epsilon\approx10$ is large [see Eq. (16a)]; second, there is strong local inhomogeneity due to the presence of large coherent structures (see Fig. 4). These coherent structures induce locally large curvature of the mean flow, which, in turn increases the rapid part of the SGS stress. In our case, the mean velocity profile is obtained by using a ''plane averaging'' procedure. The important effect of the local streamwise inhomogeneity on $\langle\tau_{11}^{\mathrm{Rapid}}\rangle$ is reduced by averaging in the streamwise direction over multiple periods of the coherent structures. If ''phase averaging'' is introduced, such as that used by O'Neil and Meneveau,[19] to obtain the local streamwise inhomogeneity, then the effect

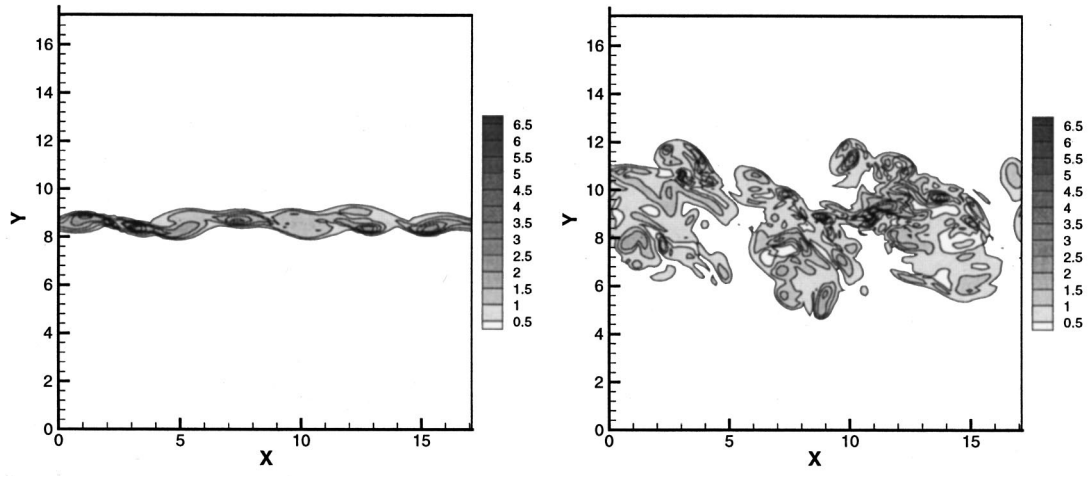

FIG. 4. Vorticity contours in the x-y plane. Left: time step=500, $t^*=236$; Right: time step=2500, $t^*=1089$.

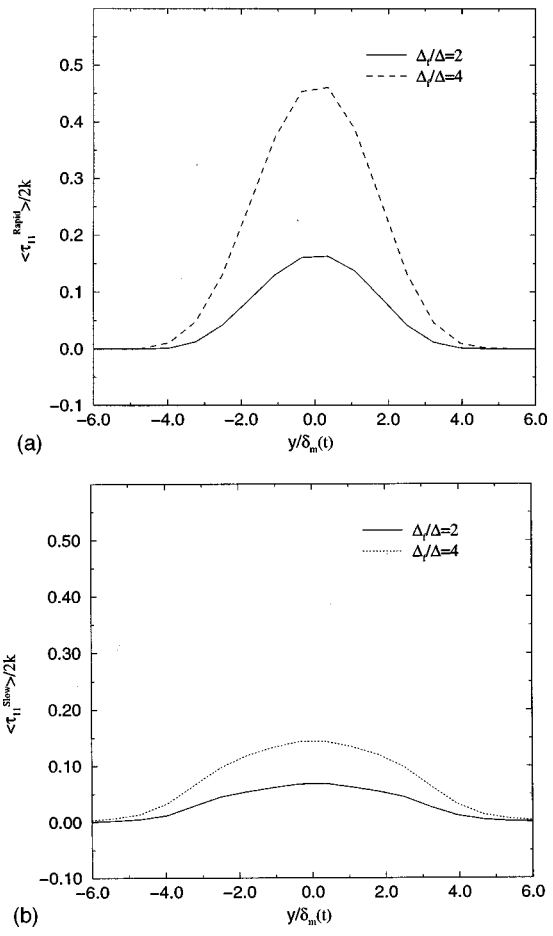

FIG. 5. (a) Normalized mean SGS stress, $\langle \tau_{11}^{\mathrm{Rapid}}/2k \rangle$, at time $t^*=236$, $\Delta_f/\Delta=2$, and 4. (b) Normalized mean SGS stress, $\langle \tau_{11}^{\mathrm{Slow}}/2k \rangle$, at time $t^*=236$, $\Delta_f/\Delta=2$, and 4.

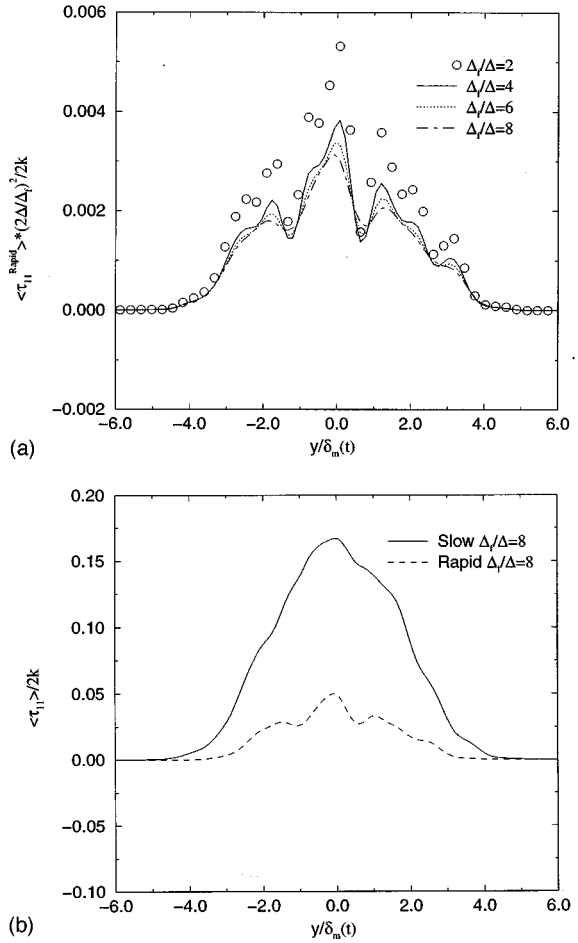

FIG. 6. (a) Normalized mean SGS stress, $\langle \tau_{11}^{\mathrm{Rapid}}/2k \rangle$, at time $t^*=1089$, $\Delta_f/\Delta=2$, 4, 6, and 8. (b) Normalized mean SGS stress, $\langle \tau_{11}^{\mathrm{Slow}}/2k \rangle$ and $\langle \tau_{11}^{\mathrm{Rapid}}/2k \rangle$, at time $t^*=1089$, $\Delta_f/\Delta=8$.

of coherent structures on $\langle \tau_{11}^{\mathrm{Rapid}} \rangle$ could be obtained. However, we do not consider coherent structures in more detail herein.

The behavior of $\langle \tau_{11}^{\mathrm{Rapid}} \rangle$ [rescaled with $(\Delta_f/\Delta)^2$] at a later stage of the mixing layer, $t^*=1089$, is given in Fig. 6(a). The scaling law, Eq. (15e), for $\langle \tau_{11}^{\mathrm{Rapid}} \rangle$ is clearly obtained in Fig. 6(a). The magnitude of the rapid part is small, but not negligible, compared to the magnitude of the slow part, $\langle \tau_{11}^{\mathrm{Slow}} \rangle$ [see Fig. 6(b)]. The small magnitude of the mean rapid part is expected, since at this stage, the flow is fully developed with equilibrium turbulence.

Another important fact is the strong anisotropy of the mean rapid SGS stress, as shown in Fig. 7(a), where $\langle \tau_{ij}^{\mathrm{Rapid}} \rangle$ is plotted (case $\Delta_f=2\Delta$, at an early stage) and Fig. 7(b) (case $\Delta_f=2\Delta$, at a later stage). In accord with the approximate expression, Eq. (15c) for $\langle \tau_{ij}^{\mathrm{Rapid}} \rangle$, the only significant component of the rapid mean SGS stress, $\langle \tau_{ij}^{\mathrm{Rapid}} \rangle$, is the 11 component. All other components are negligibly small (components 13, 23 are not plotted, they are of the same order). The sole importance of the 11 component of the mean rapid SGS stress in the temporally evolving mixing layer is a direct consequence of the simplicity of this flow; only a single component, the 12 component of the mean velocity gradient tensor is nonzero. In a more complex flow, such as the sudden expansion flow, more components of the mean rapid SGS stress would be nonzero and could have important consequences on the mean flow development. We will see later that the anisotropy of the rapid part results in a more complex energy transfer mechanism between grid and subgrid scales in the mixing layer.

It is of interest to check the anisotropy of $\langle \tau_{ij}^{\mathrm{Slow}} \rangle$. Figures 8(a)–8(b) show all components, at the early and later stages, with the filter size set to twice the grid size. At the early stage, the anisotropy is significant in both normal and shear stresses. The 12 shear component has the same order of magnitude as the diagonal components, while the two other shear components, 13 and 23, are nearly zero. Since the turbulence is still evolving in this flow, $\langle \tau_{ij}^{\mathrm{Slow}} \rangle$ is substantially influenced by the mean flow; this is an implicit effect of the mean flow gradient that is not related to physical-space filtering. At the later stage, when the turbulence is fully developed, the three diagonal components are more isotropic and are nearly equal, as shown in Fig. 8(b). Among the SGS shear stresses, the 12 shear stress is dominant and is approximately 25% of the diagonal components. The two other off-diagonal components remain negligible. In Fig. 8(c) the slow SGS shear stress $\langle \tau_{12}^{\mathrm{Slow}} \rangle$, normalized by the value of the mean shear stress $\langle u_1' u_2' \rangle$ at the centerline, is plotted at the

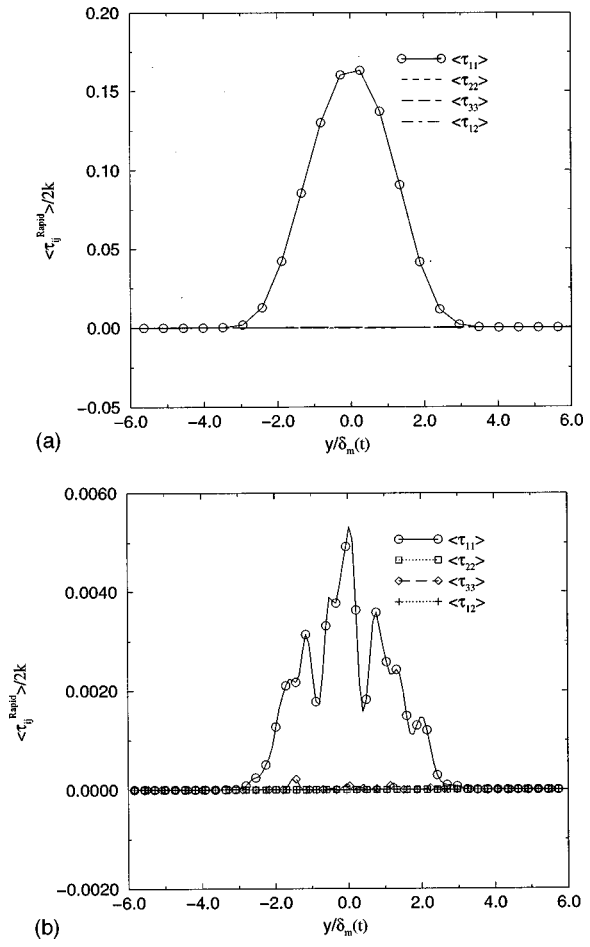

FIG. 7. (a) Normalized mean SGS stress, $\langle \tau_{ij}^{\mathrm{Rapid}}/2k \rangle$, at time $t^*=236$, $\Delta_f/\Delta=2$. (b) Normalized mean SGS stress, $\langle \tau_{ij}^{\mathrm{Rapid}}/2k \rangle$, at time $t^*=1089$, $\Delta_f/\Delta=2$.

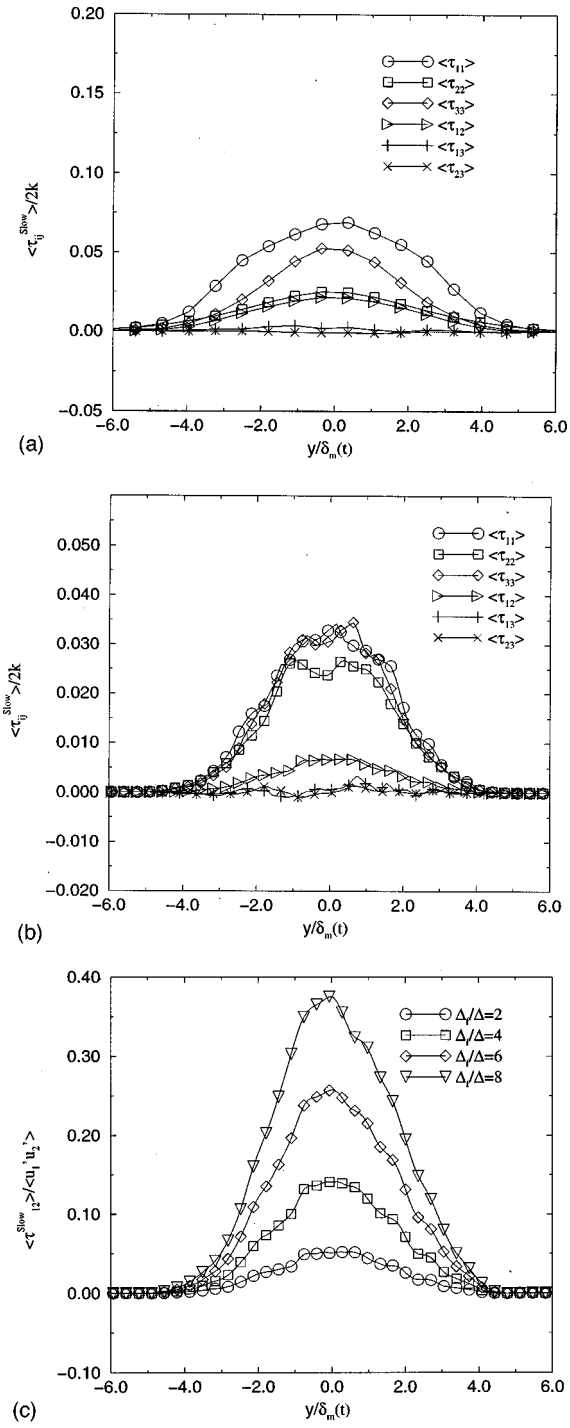

FIG. 8. (a) Normalized mean SGS stress, $\langle \tau_{ij}^{\mathrm{Slow}}/2k \rangle$, at time $t^*=236$, $\Delta_f/\Delta=2$. (b) Normalized mean SGS stress, $\langle \tau_{ij}^{\mathrm{Slow}}/2k \rangle$, at time $t^*=1089$, $\Delta_f/\Delta=2$. (c) Normalized mean slow SGS shear stress, $\langle \tau_{ij}^{\mathrm{Slow}} \rangle / \langle u_1' u_2' \rangle$, at time $t^*=1089$, $\Delta_f/\Delta=2$, 4, 6, and 8.

later stage and for different filter sizes. The importance of the SGS shear stress is clear; it varies approximately from 5% $(\Delta_f/\Delta=2)$ to 40% $(\Delta_f/\Delta=8)$ of the Reynolds-averaged shear stress when the filter size is increased. Thus the filtered scales are clearly *not* isotropic, as evidenced by the Reynolds shear stress associated with these scales. The anisotropy increases with filter size. Significant anisotropy of the SGS motion is to be expected at the filter cutoffs used in practice. Indeed, if the subgrid scales were perfectly isotropic so that the Reynolds-averaged subgrid shear stress was zero, the influence of the subgrid stress on the mean velocity field (which is through the term $\partial_j \langle \tau_{ij} \rangle$) would be zero in the turbulent mixing layer. Furthermore, physical-space filtering, since it does not perform a strict separation of scales (there is an additional smearing of scales), adds to the anisotropy induced by the mean flow. Since the nonzero SGS shear stress is important because it directly influences the mean flow, we will check later as to whether the usual SGS models can accurately capture the SGS shear stress.

b. Fluctuating SGS stress magnitude and its anisotropy. The rms value of the SGS tensor is closely related to the behavior of the small scales. Usually, in the theory of SGS modeling, the small scales are assumed to be isotropic which allows the use of the isotropic relationship concerning the energy transfer between scales. In the present case since a spatial filter is used, the fluctuating part of the SGS motion contains explicitly the mean flow [see Eq. 12(b)]; therefore, the energy transfer could deviate from isotropy.

Figures 9(a)–9(d) show the rms value of all components of the rapid and slow SGS stress tensor, at both, early and late times, for the case with $\Delta_f=2\Delta$. At both stages, the rapid SGS part shows large anisotropy; only the 11 and 12

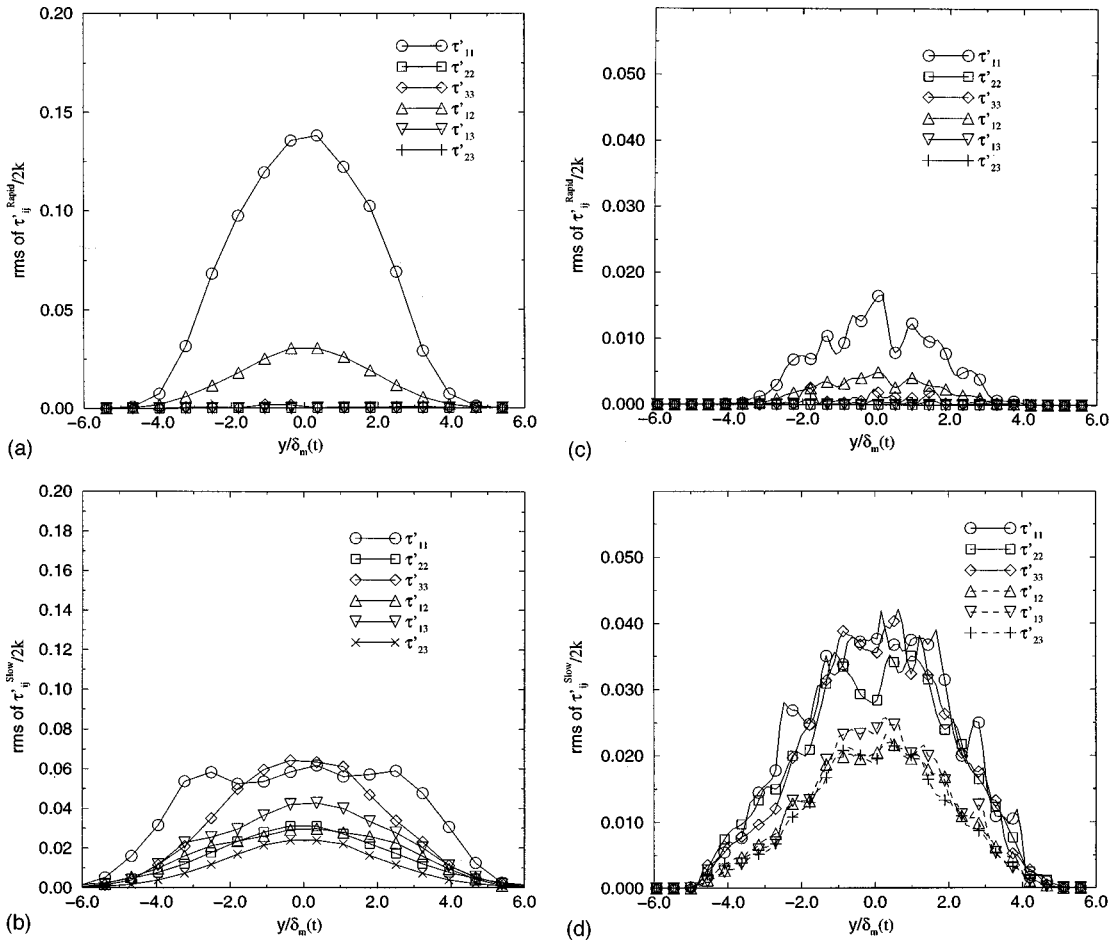

FIG. 9. (a) The rms of normalized rapid $\tau_{ij}'^{\text{Rapid}}/2k$, at time $t^*=236$, $\Delta_f/\Delta=2$. (b) The rms of normalized slow $\tau_{ij}'^{\text{Slow}}/2k$, at time $t^*=236$, $\Delta_f/\Delta=2$. (c) The rms of normalized rapid $\tau_{ij}'^{\text{Rapid}}/2k$, at time $t^*=1089$, $\Delta_f/\Delta=2$. (d) The rms of normalized slow $\tau_{ij}'^{\text{Slow}}/2k$, at time $t^*=1089$, $\Delta_f/\Delta=2$.

components are nonzero. At the early stage, all components of the rms slow SGS stress are of the same order, but are not isotropic and are smaller than the corresponding value of the rapid SGS rms. At the later stage, the rms of the normal components of the slow SGS tensor are equal and the rms of the shear components are also equal. The rms value of the rapid SGS is smaller than that of the slow component, but is significant: $\tau_{11}'^{\text{Rapid}}$ is nearly 35% of $\tau_{11}'^{\text{Slow}}$ and $\tau_{12}'^{\text{Rapid}}$ is about 30% of $\tau_{12}'^{\text{Slow}}$. The rms of the individual components of the total SGS stress (rapid+slow), even within fully developed, equilibrium turbulence (a later stage), are unequal.

Once again, the influence of the mean flow clearly appears, and is strongest at the early stage.

c. Summary. As long as the mean flow has a nonzero gradient and a spatial filter is used, there exists a rapid component of the SGS stress that cannot be ignored. In the mixing layer, the mean rapid component is especially large during the early stage of the evolution [compare Fig. 5(a) with Fig. 5(b)], in agreement with the approximate scalings derived in Sec. II D. The rapid component is strongly anisotropic in response to the mean flow. This result is consistent with and helps explain the recent finding of O'Neil and Meneveau.[19] In their study of the SGS properties in a high-Reynolds number turbulent wake using a Gaussian filter in physical space, they showed that coherent structures (the Von-Karman street) strongly correlate with the SGS stress and make the isotropy of the subgrid scales doubtful. We confirm here that mean flow gradients can lead to anisotropy of the SGS stress tensor. In the later, fully developed stage, although the mean rapid part is small, the rms of the rapid part is substantial suggesting that the rapid part could have a significant contribution to the SGS energy transfer. In the next section, the influence of the anisotropy (in both normal and shear components) of the SGS stress and the role of the rapid SGS stress with respect to the energy transfer is examined.

2. Energy transfer analysis

As pointed out in Sec. II E, the contraction of τ_{ij} by S_{ij} gives the energy transfer between different GS and SGS motions. Here, we compare the rapid SGS contribution to the slow SGS one. Recall that a positive value of the energy transfer term, $-\langle \tau_{ji} S_{ij}^{<} \rangle$, implies dissipation or forward transfer of energy while a negative value refers to backward transfer of energy. Recall also that the spherical tensor is not subtracted in our case. First, we consider the case at a later stage, $t^*=1089$. Since the turbulence is fully developed at this stage, it is easier to interpret the energy transfer mechanism. At the early stage, since the turbulence is in a strongly

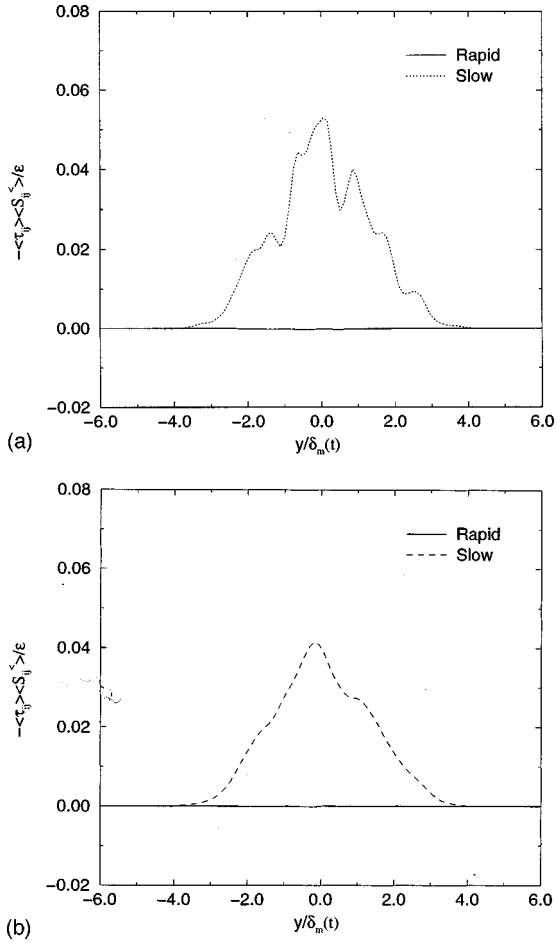

FIG. 10. (a) Energy transfer by the mean SGS stress, $-\langle\tau_{ji}^{\text{Rapid}}\rangle\langle S_{ij}^{<}\rangle/\epsilon$ *and* $-\langle\tau_{ji}^{\text{Slow}}\rangle\langle S_{ij}^{<}\rangle/\epsilon$, at time $t^*=1089$, $\Delta_f/\Delta=2$. (b) Energy transfer by the mean SGS stress, $-\langle\tau_{ji}^{\text{Rapid}}\rangle\langle S_{ij}^{<}\rangle/\epsilon$ *and* $-\langle\tau_{ji}^{\text{Slow}}\rangle\langle S_{ij}^{<}\rangle/\epsilon$, at time $t^*=1089$, $\Delta_f/\Delta=8$.

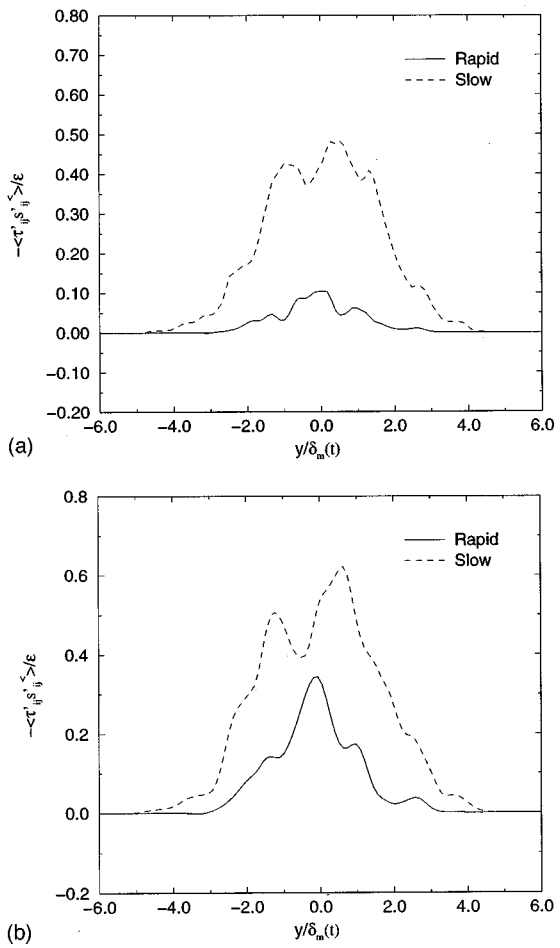

FIG. 11. (a) Subgrid energy transfer $-\langle\tau_{ji}'^{\text{Rapid}}s_{ij}'^{<}\rangle/\epsilon$ and $-\langle\tau_{ji}'^{\text{Slow}}s_{ij}'^{<}\rangle/\epsilon$, at time $t^*=1089$, $\Delta_f/\Delta=2$. (b) Subgrid energy transfer $-\langle\tau_{ji}'^{\text{Rapid}}s_{ij}'^{<}\rangle/\epsilon$ and $-\langle\tau_{ji}'^{\text{Slow}}s_{ij}'^{<}\rangle/\epsilon$, at time $t^*=1089$, $\Delta_f/\Delta=8$.

nonequilibrium state, the results are more difficult to interpret. However, notable features are identified.

a. Later stage, $t^*=1089$. Figures 10(a)–10(b) show the subgrid energy production by the mean flow, $-\langle\tau_{ji}\rangle\langle S_{ij}^{<}\rangle$, normalized by the turbulent dissipation for two filter sizes: $\Delta_f/\Delta=2$ and 8. In parallel to the observation at the tensor level comparison, the contribution of the mean rapid part, $-\langle\tau_{ji}^{\text{Rapid}}\rangle\langle S_{ij}^{<}\rangle$, is negligibly small compared to the slow part, $-\langle\tau_{ji}^{\text{Slow}}\rangle\langle S_{ij}^{<}\rangle$. But the contribution of the fluctuating rapid part of the subgrid dissipation, $-\langle\tau_{ji}'^{\text{Rapid}}s_{ij}'^{<}\rangle$, normalized by the turbulent dissipation ϵ, can be substantial, as shown in Figs. 11(a)–11(b) ($\Delta_f/\Delta=2$ and 8). Furthermore, the relative contribution of the rapid part increases with filter size.

As pointed out in the previous sections, the rapid SGS stress is highly anisotropic; the influence of its anisotropy on the grid/subgrid energy transfer is evaluated by plotting the terms $-\langle\tau_{ij}'s_{ij}'^{<}\rangle$ (no summation on index i), which occur in the GS diagonal Reynolds stresses ($\langle u_i'^{<2}\rangle$, for $i=1-3$) equations. Figures 12(a)–12(b) show the slow and rapid SGS contributions, respectively, at late time and for $\Delta_f/\Delta=8$. The slow SGS dissipation is nearly isotropic. In contrast, the high anisotropy of the rapid SGS dissipation appears clearly by the dominance of its contribution to the $\langle u_1'^{<2}\rangle$ equation. A comparison of the values of the slow and rapid SGS dissipation within the $\langle u_1'^{<2}\rangle$ equation shows that they are of the same importance. The subgrid dissipation terms in the GS shear stresses are, however, small enough to be neglected (figure not shown) for both rapid and slow components.

Once again, even for fully developed turbulence, the rapid part of the SGS stress is important because it anisotropically alters the energy transfer between grid and subgrid scales. Thus, the usual isotropic assumption for the subgrid dissipation fails. We return to this point later in the section on subgrid modeling.

b. Early stage, $t^*=236$. Since the turbulence is within a ''birth'' stage at $t^*=236$, the energy transfer mechanism is more complicated. The filter size used is twice the grid size in the following results. Figure 13 shows the respective contributions of the rapid and slow components to the SGS energy transfer, $-\langle\tau_{ji}\rangle\langle S_{ij}^{<}\rangle$. It appears that the contribution of the mean rapid part is again small, although it was shown in the section describing tensor-level results [compare Figs. 5(a) and 5(b)] that the 11 component of the mean rapid SGS stress is larger than the corresponding slow part and its energetic contribution can be neglected. This is not surprising, since the mean flow is a simple shear flow; $\langle S_{11}^{<}\rangle\approx 0$ and,

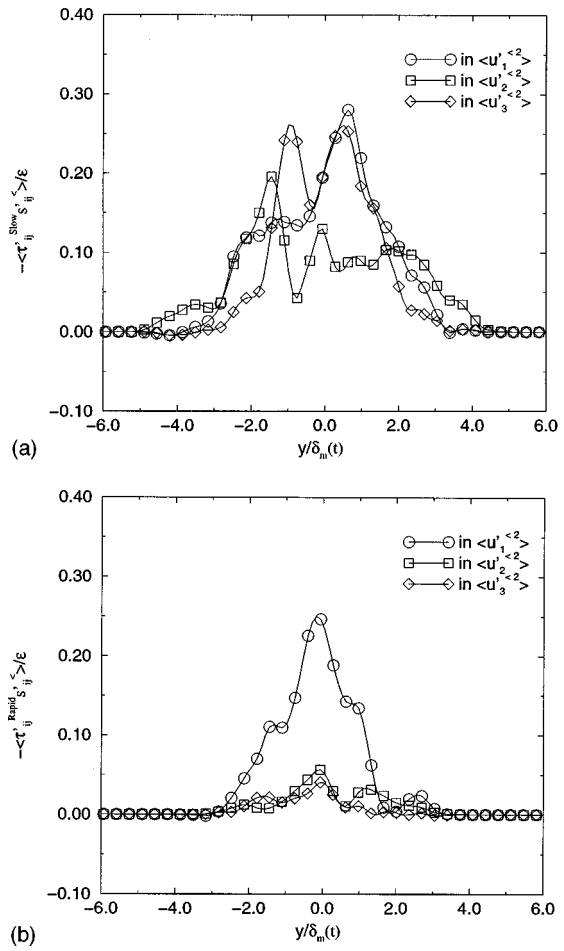

FIG. 12. (a) Subgrid energy transfer $-\langle \tau_{ji}'^{\text{Slow}} s_{ij}'^{<} \rangle / \epsilon$ in $\langle u_i'^{<2} \rangle$ equations, for $i=1-3$, at $t^*=1089$, $\Delta_f/\Delta=8$. No summation on index i is implied. (b) Subgrid energy transfer $-\langle \tau_{ji}'^{\text{Rapid}} s_{ij}'^{<} \rangle / \epsilon$ in $\langle u_i'^{<2} \rangle$ equations, for $i=1-3$, at $t^*=1089$, $\Delta_f/\Delta=8$. No summation on index i is implied.

consequently, the contribution of the 11 component to $-\langle \tau_{ji} \rangle \langle S_{ij}^{<} \rangle$ is negligible. It must be emphasized that, in other cases, like the near-wake of a bluff body or the flow with streamwise contraction, the production by the mean rapid SGS stress is potentially important.

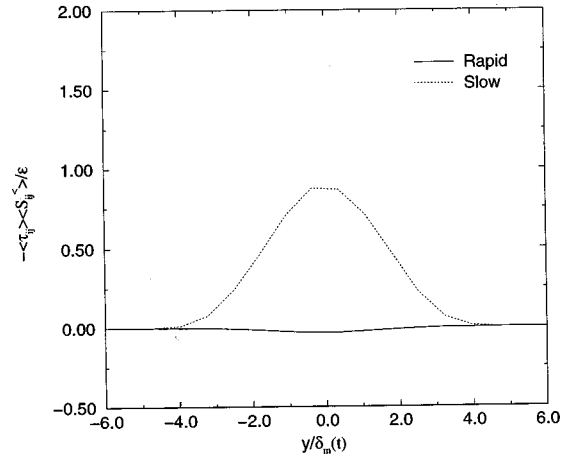

FIG. 13. Subgrid energy production by the mean flow $-\langle \tau_{ji}^{\text{Rapid}} \rangle \langle S_{ij}^{<} \rangle / P$ and $-\langle \tau_{ji}^{\text{Slow}} \rangle \langle S_{ij}^{<} \rangle / P$, at time $t^*=236$, $\Delta_f/\Delta=2$.

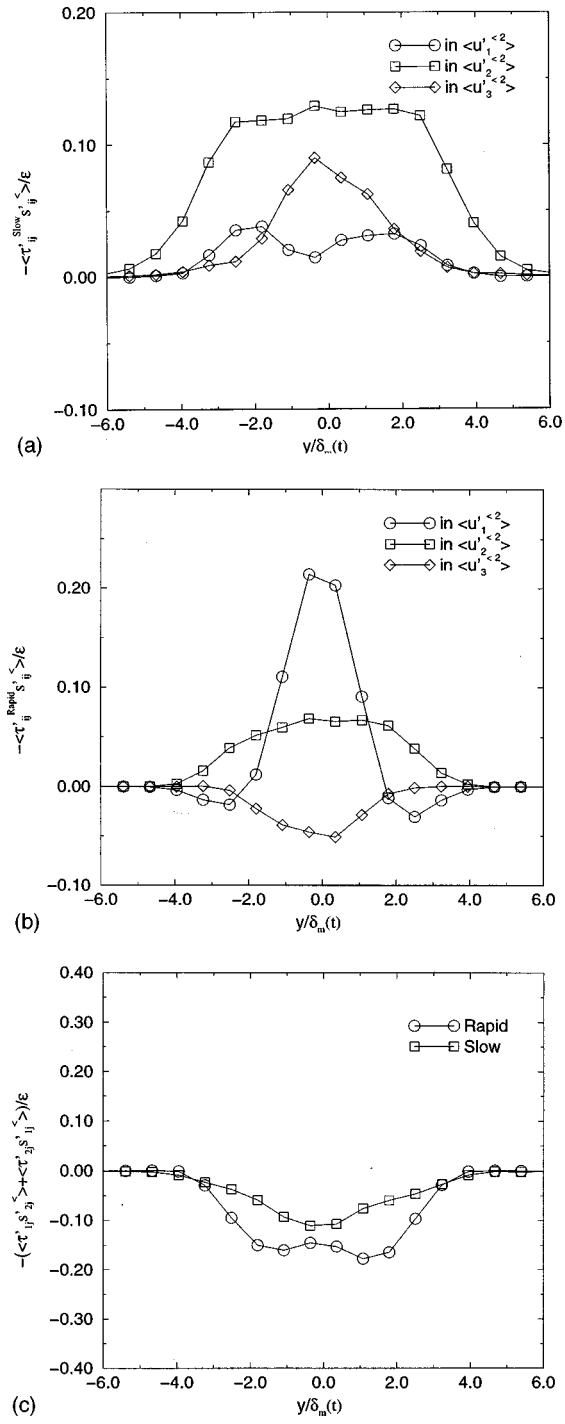

FIG. 14. (a) Subgrid energy transfer $-\langle \tau_{ji}'^{\text{Slow}} s_{ij}'^{<} \rangle / \epsilon$ in $\langle u_i'^{<2} \rangle$ equations, for $i=1-3$, at $t^*=236$, $\Delta_f/\Delta=2$. No summation on index i is implied. (b) Subgrid energy transfer $-\langle \tau_{ji}'^{\text{Rapid}} s_{ij}'^{<} \rangle / \epsilon$ in $\langle u_i'^{<2} \rangle$ equations, for $i=1-3$, at time $t^*=236$, $\Delta_f/\Delta=2$. No summation on index i is implied. (c) Subgrid energy transfer (rapid and slow) in $\langle u_1'^{<} u_2'^{<} \rangle$ equation at time $t^*=236$, $\Delta_f/\Delta=2$.

The subgrid energy transfer, $-\langle \tau_{ji}' s_{ij}'^{<} \rangle$, in each diagonal component of the GS Reynolds stress tensor ($\langle u_i'^{<2} \rangle$) is illustrated in Fig. 14(a) (slow SGS) and Fig. 14(b) (rapid SGS). First, we observe significant anisotropy, even in the slow SGS dissipation. Second, the rapid and slow contributions are of the same magnitude. Third, the contribution of

the rapid stress represents a back-transfer (the negative value of $-\langle \tau'_{ji} s'^{<}_{ij} \rangle$) in the $\langle u'^{<2}_3 \rangle$ and the $\langle u'^{<2}_1 \rangle$ equation. Regarding the shear stress, $\langle u'^{<}_1 u'^{<}_2 \rangle$, a similar back-transfer is observed on both the rapid and slow part, as shown in Fig. 14(c). Such a complex transfer mechanism is difficult to interpret but may be related to the presence of vortex breakdown during the transition to three-dimensional turbulence, as well as to the simultaneous presence of large coherent structures. To understand these particular features, we need to investigate the transition to turbulence, but this is beyond the scope of the present study.

c. Summary. The presence of the rapid SGS stress alters the subgrid transfer in an anisotropic fashion. The anisotropy is related directly to the mean flow, with the rapid part primarily contributing to the streamwise component of the subgrid transfer in the shear layer. The rapid component has a dominant influence at an early time when the turbulence is in nonequilibrium. In the case of later-time, equilibrium turbulence, the rapid contribution to the SGS energy transfer increases with filter size and the rapid contribution to the streamwise SGS transfer is comparable to that of the slow term [compare Fig. 12(b) with Fig. 12(a)]. In the next section, when we evaluate popular subgrid models, attention is focused on the ability of these models to account for the anisotropy induced into the grid/subgrid energy transfer by the rapid SGS stress.

IV. EVALUATION OF SUBGRID MODELS

From the discussion of the previous sections, it is clear that, through the rapid part, the mean velocity gradient directly affects the SGS stress tensor subgrid stress tensor and the associated energy transfer to the small scales. The question that then arises is whether SGS modeling has to explicitly account for the effect of the mean velocity gradient manifested by the rapid SGS stress. Here, we evaluate the ability of existing SGS models to represent the distinct properties of the rapid and slow parts of the SGS tensor. The comparison is limited to two popular models in LES applications: the eddy viscosity Smagorinsky model and the Galilean invariant scale-similarity model. There is no separate term explicitly depending on the mean velocity gradient, though there is an implicit dependence in both models. Although, as pointed out previously,[8,9,19] the Galilean-invariant scale-similarity model has a high correlation with the SGS stress and also allows backscatter, its use in a practical computation can lead to numerical instability. Therefore, a combination of these two models (the mixed model) is used in practice with the Smagorinsky component added for numerical stability to the scale-similarity model. However, it is not clear if there is an additional physical reason for retaining both scale-similarity and eddy viscosity components in a SGS model.

In accord with previous investigations, our study also gives a high value of the correlation coefficients between the exact SGS stress and the scale-similarity model (about 0.9 for both rapid and slow components). We do not present detailed results about the correlation coefficients at the tensor level between the model predictions and exact values of the SGS stress. Instead model validation is performed with respect to the rapid and slow components of the SGS stress. Attention is focused on whether the anisotropic nature of the energy transfer mechanism and the high value of the SGS shear stress associated with the limited resolution possible in practical LES can be correctly captured by the two models studied here.

A. Subgrid models

The Smagorinsky model represents the deviatoric part of τ_{ij} as follows:

$$\tau_{ij_{\text{Smag}}} = -2\nu_t S^{<}_{ij}, \tag{23}$$

where $S^{<}_{ij}$ is the strain rate tensor of the resolved grid-scale motion and ν_t is an ''eddy viscosity,'' defined by

$$\nu_t = (C_s \Delta')^2 \sqrt{2 S^{<}_{ij} S^{<}_{ij}}. \tag{24}$$

Here, C_s is a constant (its value is usually about 0.15), and Δ' denotes an ''effective'' filter size. This model correlates poorly with the SGS tensor, as noted in the literature, but it is purely dissipative and, thus, assumes one of the essential functions of a SGS model,

The scale-similarity model is defined as:

$$\tau_{ij} = \alpha L_{ij} = \alpha((u^{<}_i u^{<}_j)^{<} - u^{\ll}_i u^{\ll}_j). \tag{25}$$

The second filtering operation is done with a ''test'' filter that is the same as the original ''grid'' filter. The adjustable constant is chosen to be $\alpha = 1$ here. The rapid and slow components of the modeled stresses will be compared with corresponding exact values from the DNS. The slow part of the Smagorinsky model is obtained by using the fluctuating strain rate instead of the total strain rate on the rhs of Eq. (23), as well as on the rhs of Eq. (24) when calculating the required eddy viscosity. The slow part of the scale-similarity model is obtained using the fluctuating velocity instead of the total velocity on the rhs of Eq. (25). The rapid part of both the Smagorinsky and scale-similarity model is obtained by subtracting the slow part from the model prediction for the total SGS stress.

B. A comparison with DNS results

At the early stage, since the turbulence is not fully developed, the Smagorinsky model coefficient is not well defined. Therefore, a quantitative comparison with the Smagorinsky model is not performed with the early-time data. For the scale-similarity model, a comparison is done using both, the early- and late-time datasets. The important yardsticks for the comparison are the following: first, the value of the SGS shear stress, and second, the anisotropic energy transfer between the mean velocity/grid-scale fluctuation/subgrid-scale fluctuation.

Figures 15(a)–15(d) show the modeled (both Smagorinsky and scale-similarity models) and exact values of the total SGS shear stress, $\langle \tau_{12} \rangle$, normalized by the centerline value of $\langle u'_1 u'_2 \rangle$, for $\Delta_f/\Delta = 2$, 4, 6, and 8, at a late time. It appears that the Smagorinsky model largely underestimates this quantity, and better agreement is obtained with the scale-

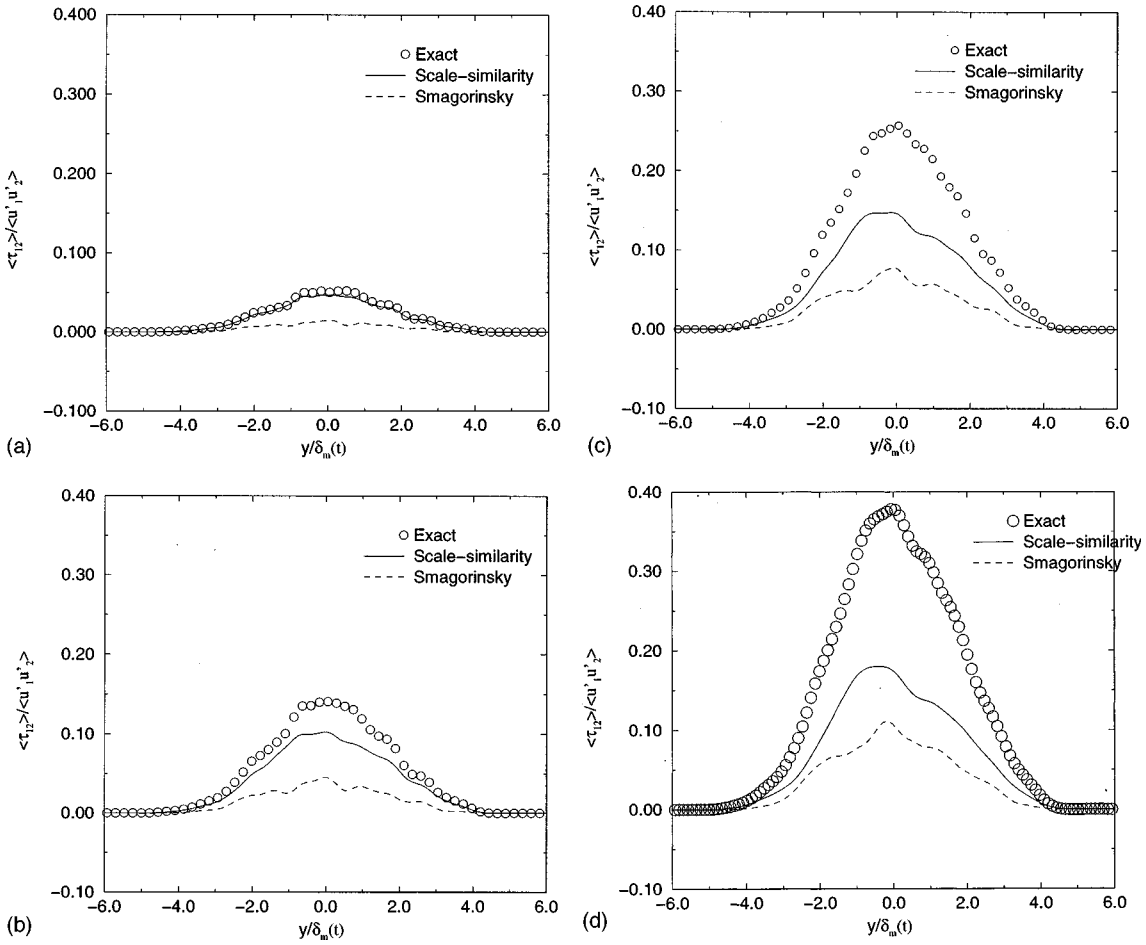

FIG. 15. (a) A comparison between modeled and exact total SGS shear stress, at time $t^*=1089$, $\Delta_f/\Delta=2$. (b) A comparison between modeled and exact total SGS shear stress, at time $t^*=1089$, $\Delta_f/\Delta=4$. (c) A comparison between modeled and exact total SGS shear stress, at time $t^*=1089$, $\Delta_f/\Delta=6$. (d) A comparison between modeled and exact total SGS shear stress, at time $t^*=1089$, $\Delta_f/\Delta=8$.

similarity model. However, when the filter size increases, differences with the exact DNS results also increase. It appears that, with decreasing LES resolution, α in Eq. (26) would have to be progressively larger for the scale-similarity model to match the exact $\langle \tau_{12} \rangle$. This is consistent with the recent study of Cook.[25] These results are also consistent with a conclusion from Vreman *et al.*[26] in their LES study of the turbulent mixing layer, that the mixed model (scale similarity plus Smagorinsky) gives a better shear layer growth rate than the Smagorinsky model by itself.

Figures 16(a) and 16(b) evaluate the ability of the scale-similarity model to represent the rapid and slow parts of the exact subgrid energy transfer terms, $-\langle \tau_{ij}' s_{ij}'^{<} \rangle$, in the SGS turbulent kinetic energy equations. The energy transfers are evaluated using the DNS data at late time, and for $\Delta_f/\Delta = 6$. The coefficient used for the Smagorinsky constant is 0.15. The scale-similarity model does a good job in representing the rapid part as shown in Fig. 16(a) while it performs poorly with respect to the slow part, as shown in Fig. 16(b). The energy transfers predicted by the Smagorinsky model are compared with the exact values in Figs. 16(c)–16(d). The rapid subgrid transfer is not captured by the Smagorinsky model, as shown in Fig. 16(c) while the slow energy transfer is well represented, as shown in Fig. 16(d). Thus, it appears that the rapid part of the energy transfer is better represented by the scale-similarity model while the Smagorinsky model is better for capturing the energy dissipation associated with the slow part.

At the early stage, the anisotropic energy transfer is more important due to the large rapid SGS stress. Figure 17(a) [respectively, (17b)] shows the rapid (respectively, slow) contributions to the $\langle u_1'^{<2} \rangle$ and $\langle u_2'^{<2} \rangle$ equations, while Fig. 17(c) shows the rapid and slow contributions to the transport equation for the GS shear stress $\langle u_1'^{<} u_2'^{<} \rangle$, at early time, and for $\Delta_f/\Delta = 2$. It is remarkable that the anisotropy in the component energy transfers as well as the reverse energy transfer are captured by the scale-similarity model. It should be noted that the Smagorinsky model would not be able to predict the reverse energy transfer.

From the above discussion it is clear that the mixed model is better suited for complex inhomogeneous, anisotropic turbulent flows. The scale-similarity part represents the anisotropic energy transfer induced by the mean velocity gradient through the rapid part as well as reverse energy transfer, while the Smagorinsky part represents well the subgrid dissipation associated with the slow part. Thus, there is a physically based reason for including both, the scale-

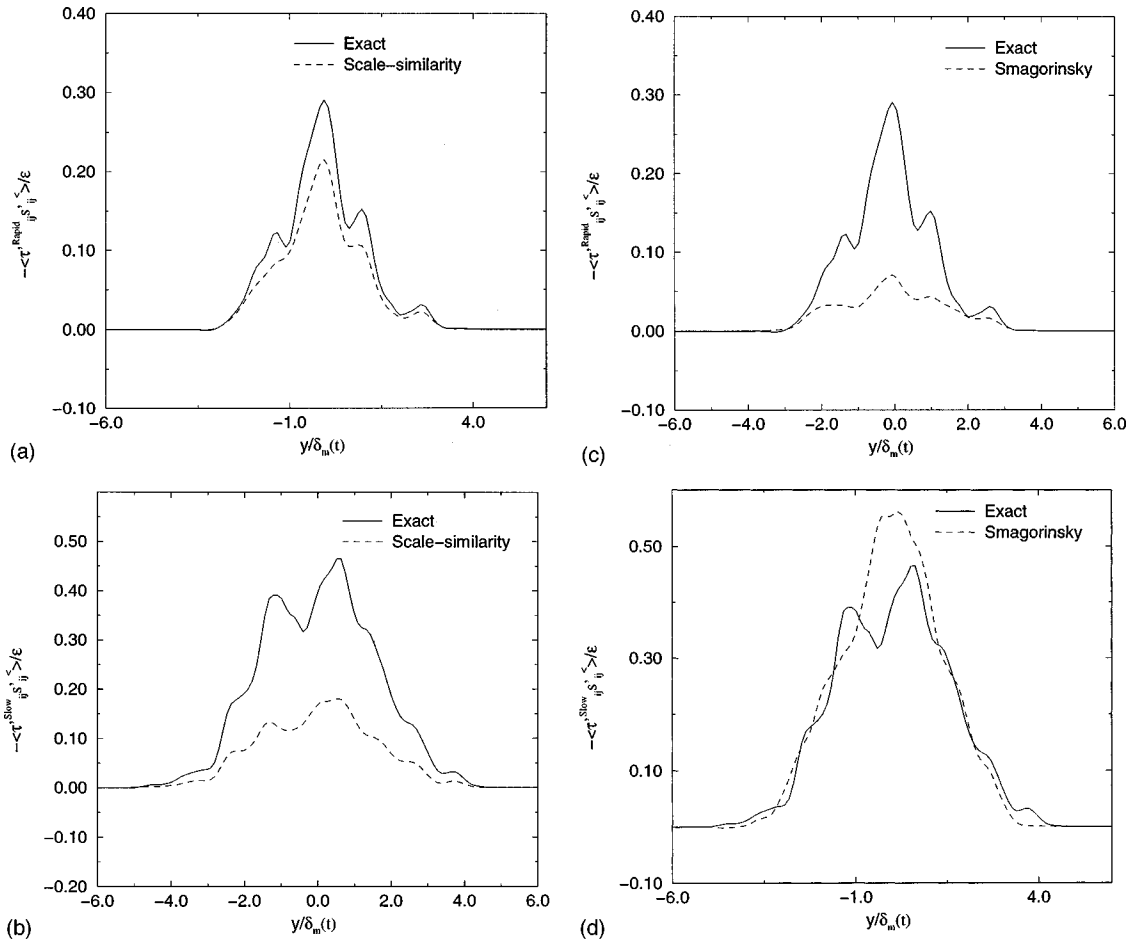

FIG. 16. (a) A comparison with the scale-similarity (L_{ij}) model. Rapid subgrid energy transfer terms, $-\langle \tau_{ij}'^{\mathrm{Rapid}} s_{ij}'^{<} \rangle$, at time $t^*=1089$, $\Delta_f/\Delta=6$. (b) A comparison with the scale-similarity (L_{ij}) model. Slow subgrid energy transfer terms, $-\langle \tau_{ij}'^{\mathrm{Slow}} s_{ij}'^{<} \rangle$, at time $t^*=1089$, $\Delta_f/\Delta=6$. (c) A comparison with the Smagorinsky model. Rapid subgrid energy transfer terms, $-\langle \tau_{ij}'^{\mathrm{Rapid}} s_{ij}'^{<} \rangle$, at time $t^*=1089$, $\Delta_f/\Delta=6$. (d) A comparison with the Smagorinsky model. Slow subgrid energy transfer terms, $-\langle \tau_{ij}'^{\mathrm{Slow}} s_{ij}'^{<} \rangle$, at time $t^*=1089$, $\Delta_f/\Delta=6$.

similarity and the Smagorinsky parts, as is done in the mixed model. It should be noted that the Smagorinsky constant is set to the value of $C_s=0.15$, which is appropriate for the mixing layer. It may be necessary to use the dynamic Smagorinsky model to predict the slow part of the SGS dissipation in more general flows.

V. INFLUENCE OF THE MEAN FLOW IN THE CASE OF A HOMOGENEOUS SPATIAL FILTER

In this section we consider the situation when a homogeneous filter is used in the mixing layer, i.e., when the top hat filter is applied only in the homogeneous flow directions *x* and *z*. The resulting SGS tensor does not explicitly contain the mean flow; thus, there is no rapid part. However, there exists an effect of the mean velocity on the SGS energy transfer that is *implicit*. It is of interest to compare such filtering to the study of Haertel *et al.*,[23] which uses an ideal spectral-space filter without leading to a rapid SGS component, in particular, their analysis of the SGS energy transfer mechanism. It should be noted that our study uses physical-space filtering while that of Haertel *et al.*[23] uses a spectral-space ideal filter. Although the pipe flow and the channel flow used in the study of Haertel *et al.*[23] are different from the shear layer studied here, some similarities in the influence of mean shear on the SGS stress may be anticipated. In the near-wall buffer region, the turbulence is in a nonequilibrium stage with the turbulence production much larger than the dissipation; therefore, an analogy with the early stage of a mixing layer may be drawn. In the log layer, the turbulence is in equilibrium with production equal to dissipation, which could lead to similarities with the later stage of the mixing layer when the turbulence is fully developed.

Figures 18(a) and 18(b) show the energy transferred from the mean flow to the subgrid scales, $-\langle \tau_{ij} \rangle \langle S_{ij}^{<} \rangle$, as well as the nonlinear energy transfer between turbulent scales, $-\langle \tau_{ij}' s_{ij}'^{<} \rangle$, for the later stage and for $\Delta_f/\Delta=2$ and 4. The flux from the mean flow is significantly smaller than the flux between turbulent scales. This result is in qualitative agreement with the results in the region far from the wall observed by Haertel *et al.*,[23] and also with those of Domaradzki *et al.*,[18] who show that the direct transfer by the mean flow to the subgrid-scale fluctuations is relatively small. Model predictions of the nonlinear energy transfer have been discussed previously. The energy transfer, $-\langle \tau_{ij} \rangle \langle S_{ij}^{<} \rangle$, associated with the mean SGS stress, is compared with model

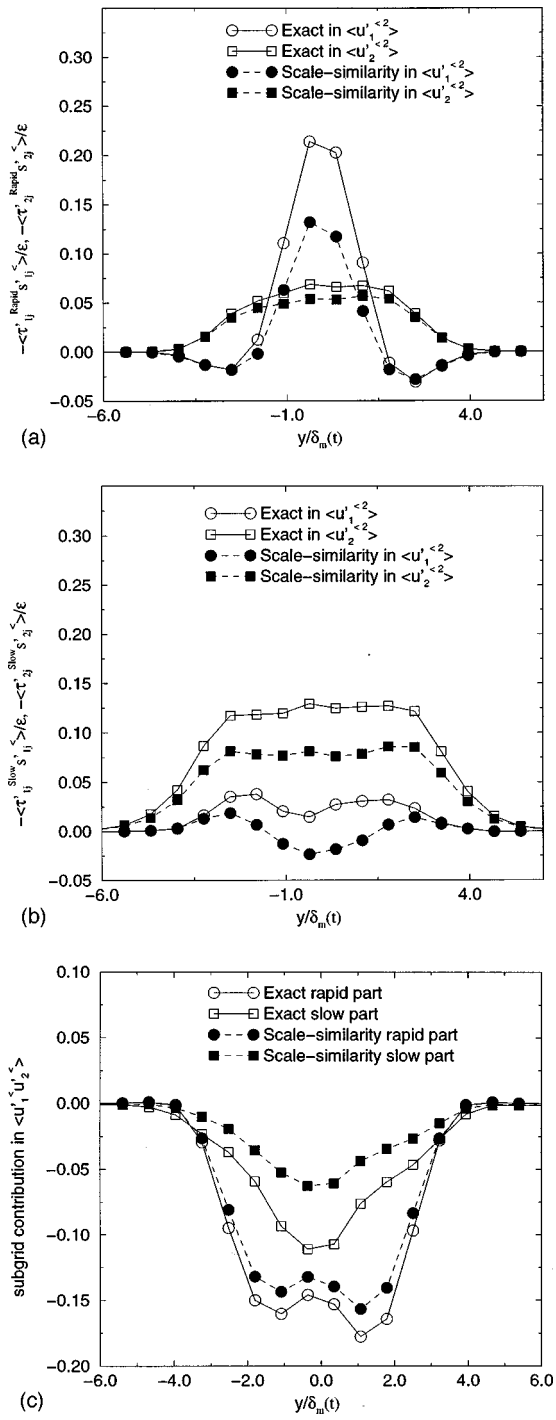

FIG. 17. (a) A rapid contribution to energy transfer in $\langle u_1'^{<2}\rangle$ and $\langle u_2'^{<2}\rangle$ equations, at time $t^*=236$, $\Delta_f/\Delta=2$. A comparison with the scale-similarity model (L_{ij}). (b) A slow contribution to energy transfer in $\langle u_1'^{<2}\rangle$ and $\langle u_2'^{<2}\rangle$ equations, at time $t^*=236$, $\Delta_f/\Delta=2$. A comparison with the scale-similarity model (L_{ij}). (c) Rapid and slow contributions to energy transfer in the $\langle u_1'^{<}u_2'^{<}\rangle$ equation, at time $t^*=236$, $\Delta_f/\Delta=2$. A comparison with the scale-similarity model (L_{ij}).

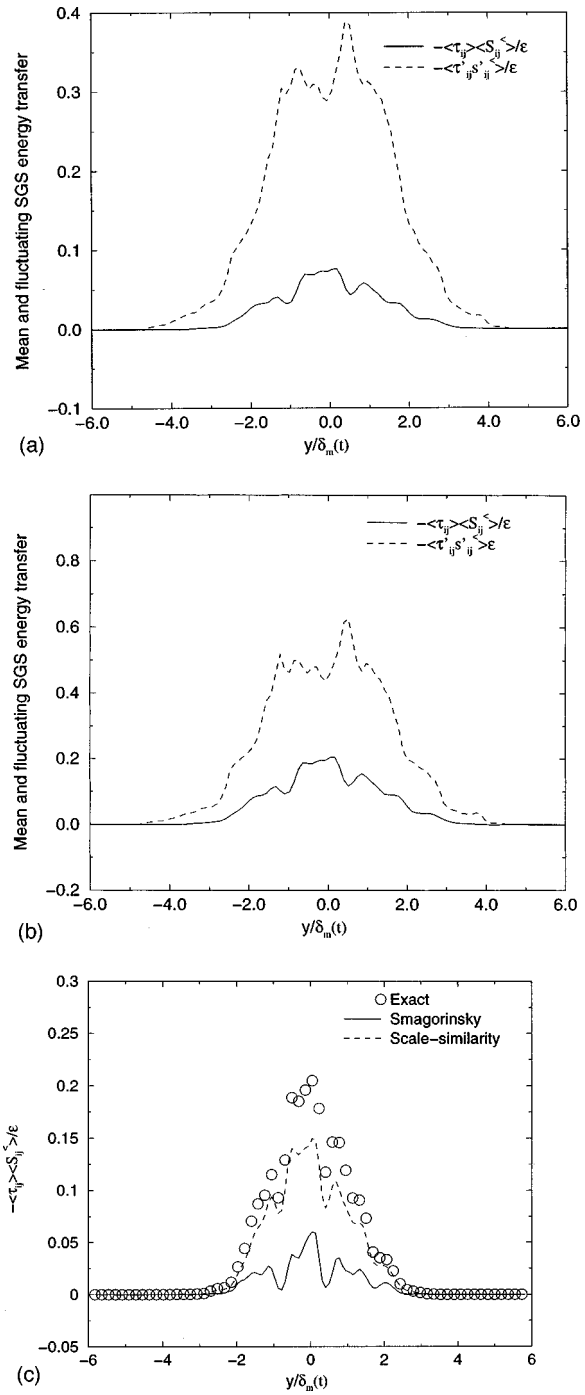

FIG. 18. (a) Energy transfer from mean flow to the SGS, $-\langle\tau_{ij}\rangle\langle S_{ij}^{<}\rangle/\epsilon$, and energy transfer between turbulence scales, $-\langle\tau_{ij}'s_{ij}'^{<}\rangle/\epsilon$, at $t^*=1089$, $\Delta_f/\Delta=2$. (b) Energy transfer from mean flow to the SGS, $-\langle\tau_{ij}\rangle\langle S_{ij}^{<}\rangle/\epsilon$, and energy transfer between turbulence scales, $-\langle\tau_{ij}'s_{ij}'^{<}\rangle/\epsilon$, at $t^*=1089$, $\Delta_f/\Delta=4$. (c) Evaluation of model predictions of energy transfer from mean flow to the subgrid scales at $t^*=1089$, $\Delta_f/\Delta=4$.

predictions in Fig. 18(c). The scale-similarity model performs better than the Smagorinsky model

Figure 19 shows the energy transfer between large and small turbulent scales for each normal stress component, $-\langle\tau_{ij}'s_{ij}'^{<}\rangle$ (without summation on index i) in the fully developed mixing layer. The energy transfer can be compared with corresponding quantities obtained when filtering is applied in all three directions. The transfer is similar to that associated with the slow part of the SGS tensor [see Fig. 12(a)], with no evidence of the strong anisotropy associated with the rapid component [see Fig. 12(b)]. Furthermore, the quasi-isotropy of the SGS energy transfer agrees with the results of Haertel *et al.*[23] in the region far from the wall.

At the early stage, the mean flow plays a dominant role

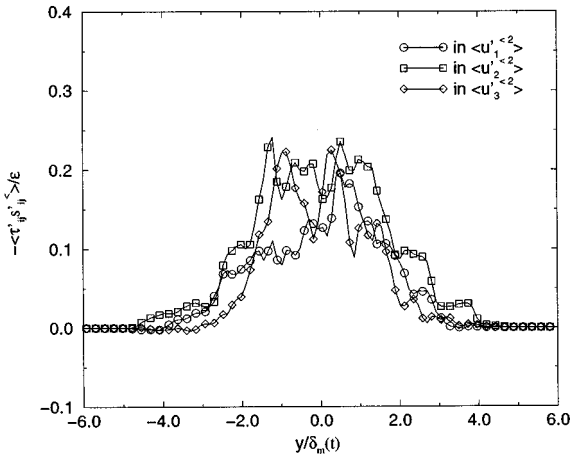

FIG. 19. Subgrid energy transfer $-\langle \tau'_{ji} s'^{<}_{ij} \rangle / \epsilon$ in $\langle u'^{<2}_i \rangle$ equations, for $i=1-3$, at $t^*=1089$, $\Delta_f/\Delta=2$. No summation on index i is implied.

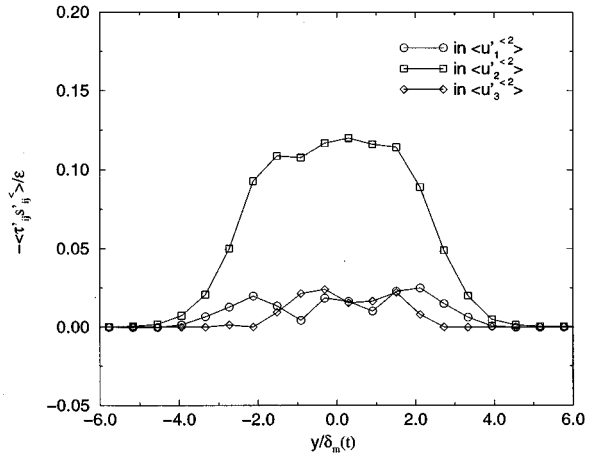

FIG. 21. Subgrid energy transfer $-\langle \tau'_{ji} s'^{<}_{ij} \rangle / \epsilon$ in $\langle u'^{<2}_i \rangle$ equations, for $i=1-3$, at an early stage, $t^*=236$, $\Delta_f/\Delta=2$. No summation on index i is implied.

in the energy transfer mechanism, as shown in Fig. 20, where $-\langle \tau_{ij} \rangle \langle S^{<}_{ij} \rangle$ and $-\langle \tau'_{ij} s'^{<}_{ij} \rangle$ are compared for $\Delta_f/\Delta=2$. In agreement with the results in the near-wall region of Haertel *et al.*,[23] the mean contribution, $-\langle \tau_{ij} \rangle \langle S^{<}_{ij} \rangle$, is larger than the fine-scale contribution, $-\langle \tau'_{ij} s'^{<}_{ij} \rangle$. When $-\langle \tau'_{ij} s'^{<}_{ij} \rangle$ (no summation on index i) is plotted for different Reynolds stress components (see Fig. 21), in agreement with the observation of Haertel *et al.*[23] and also with previous results concerning the slow part in the case where the filter is applied in all three directions [see Fig. 14(a)], a strong anisotropy in the energy transfer mechanism clearly appears. However, unlike the other study, which uses the spectral cutoff filter, no backward transfer is observed with the physical-space filter used here. This is consistent with an analytical prediction made by Leslie and Quarini,[12] experimentally observed by Liu *et al.*[8] and numerically confirmed by Piomelli *et al.*,[27] that is, physical-space filtering significantly reduces the amount of backward transfer with respect to spectral-space filtering.

In summary, when the filter is applied only in the homogeneous flow directions, the results concerning the SGS energy transfer mechanism agree qualitatively well with previous studies using the spectral cutoff filter in the literature because the rapid component is now absent. Furthermore, it is demonstrated that the early-time, nonequilibrium turbulence in the shear layer has strongly anisotropic SGS energy transfer analogous to that observed in near-wall turbulence by Haertel *et al.*,[23] while fully developed turbulence in the shear layer has a substantially more isotropic energy exchange between grid and subgrid scales, similar to that in equilibrium, log-layer turbulence.

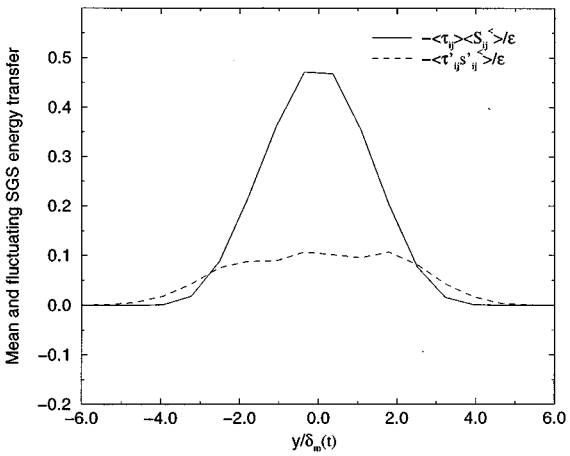

FIG. 20. Energy transfer from mean flow to the SGS, $-\langle \tau_{ij} \rangle \langle S^{<}_{ij} \rangle / \epsilon$, and energy transfer between turbulence scales, $-\langle \tau'_{ij} s'^{<}_{ij} \rangle / \epsilon$, at early stage, $t^*=236$, $\Delta_f/\Delta=2$.

VI. CONCLUDING REMARKS

Subgrid-scale modeling in the case of inhomogeneous turbulent flows is considered. By definition, the mean velocity has a nonuniform gradient in the direction of inhomogeneity. Filtering in the inhomogeneous direction is necessary in the LES of such flows because a computational grid sufficiently fine to resolve the smallest spatial scale of the turbulence in that direction is not practical. Inhomogeneity does not permit the use of the spectral cutoff filter in that direction and physical-space filtering provides a simple alternative.

In this paper we focus on the properties of the SGS stress linked with the presence of mean velocity gradients. It is shown that, in addition to the classical SGS stress tensor due to the fluctuating velocity, a contribution that is explicitly connected to the mean velocity gradient is also present. By analogy to the decomposition into rapid and slow parts of the pressure–strain correlation in Reynolds-averaged turbulence modeling, a rapid SGS stress, which depends explicitly on the mean velocity gradient, and a slow SGS stress that does not are defined. Any change in the mean velocity is instantaneously reflected in the rapid SGS stress. The rapid part induces not only significant anisotropy in the SGS stress but also alters the energy transfer between grid and subgrid scales of turbulence. Analysis of these two SGS stress components using a Taylor expansion shows that the magnitude of the rapid part can be comparable to the slow part in two situations: first, when the turbulence is not in an equilibrium

state, that is, $P/\epsilon > O(1)$, and second, in equilibrium turbulence when the resolution is such that the filter size is not much smaller than the integral length scale of turbulence. *A priori* tests are performed using an existing direct numerical simulation database of the temporally evolving turbulent mixing layer. Quantitative and qualitative agreement between numerical results and the analysis is obtained. The numerical results also show back-transfer of energy associated with the rapid SGS stress.

When the filter is applied solely in the homogeneous flow directions, the rapid component of the SGS stress is absent. However, there is an implicit effect of the mean velocity gradient on the SGS stress, which, from DNS of the temporally evolving mixing layer, is found to be large at the early-time, transitional stage and small during the late-time stage corresponding to equilibrium turbulence. The results concerning the SGS energy transfer mechanism agree qualitatively well with previous studies using the spectral cutoff filter in the literature. Furthermore, it is demonstrated that the early-time, nonequilibrium turbulence in the shear layer has strongly anisotropic SGS energy transfer analogous to that observed in near-wall turbulence, while fully developed turbulence in the shear layer has a substantially more isotropic energy exchange between grid and subgrid scales in equilibrium, similar to that in equilibrium, log-layer turbulence.

It is of interest to determine if existing models, which do not have a separate explicit dependence on the mean velocity, can represent the effect of the rapid SGS stress. Two popular SGS models, the scale-similarity and the Smagorinsky model, have been considered. Tests are done for the energy transfer and for the shear stress, for both the rapid and slow parts. It is found that the scale-similarity model reproduces the anisotropic and backscatter features of the energy transfer mechanism associated with the rapid part, while the transfer related to the slow part, usually the purely dissipative forward energy transfer, is adequately captured by the Smagorinsky model. During the *a priori* test, it is also found that the subgrid shear stress is substantial for filter sizes that are used in practice. An important strength of the scale-similarity model is that its predictions of the subgrid shear stress are better than the Smagorinsky model. These findings may explain why LES with the combination of the two subgrid-scale models, i.e., the mixed model, has been successful in different situations

In the present test case of the temporally evolving mixing layer, even though the mean flow is one-dimensional and not strongly inhomogeneous, the effect of the rapid part is still manifest. It should be noted that, based on the present work, the contribution of the rapid part of the SGS stress tensor and the importance of the scale-similarity component of the SGS stress model can be expected to increase in the following examples of nonequilibrium turbulence: a rapid distortion flow and a flow with local inhomogeneity, that is, inhomogeneity induced by local, large-scale coherent structures. For example, a recent experimental study[28] found significant effects of the mean flow on the SGS stress during rapid axisymmetric expansion of initially isotropic turbulence, which could not be represented with the Smagorinsky model. Similarly, an experimental study of a high-Reynolds number cylinder wake,[19] a flow with local inhomogeneity, found that the SGS dissipation obtained by streamwise filtering depended strongly on large-scale coherent structures when conditionally averaged and, furthermore, while the similarity model was able to capture this phenomenon the Smagorinsky model was not.

ACKNOWLEDGMENTS

The support of AFOSR Grant No. F49620-96-1-0106 is acknowledged. This work was done when L. Shao was a visitor in the Department of AMES, University of California, San Diego. Special thanks are due to CNRS and NATO for providing financial support, in part, for this visit.

[1] M. Lesieur and O. Métais, ''New trends in large-eddy simulations of turbulence,'' Annu. Rev. Fluid Mech. **28**, 45 (1996).
[2] P. Moin, ''Progress in large eddy simulation of turbulent flows,'' AIAA Paper No. 97-0749, 1997.
[3] U. Piomelli and J. R. Chasnov, ''Large eddy simulations: theory and applications,'' in *Turbulence and Transition Modelling*, edited by M. Hallback, D. S. Henningson, A. V. Johannson, and P. H. Alfredsson (Kluwer, Dordrecht, 1996).
[4] A. Leonard, ''On the energy cascade in large-eddy simulations of turbulent fluid flows,'' Adv. Geophys. **18**, 237 (1974).
[5] U. Piomelli, P. Moin, and J. H. Ferziger, ''Model consistency in large eddy simulation of turbulent channel flows,'' Phys. Fluids **31**, 1884 (1988).
[6] M. Germano, U. Piomelli, P. Moin, and W. H. Cabot, ''A dynamic subgrid-scale eddy viscosity model,'' Phys. Fluids A **3**, 1760 (1991).
[7] J. Bardina, J. H. Ferziger, and W. C. Reynolds, ''Improved turbulence models based on LES of homogeneous incompressible turbulent flows,'' Department of Mechanical Engineering Report No. TF-19, Stanford, 1984.
[8] S. Liu, C. Meneveau, and J. Katz, ''On the properties of similarity subgrid-scale models as deduced from measurements in a turbulent jet,'' J. Fluid Mech. **275**, 83 (1994).
[9] M. V. Salvetti and S. Banerjee, ''*A priori* tests of a new dynamic subgrid-scale model for finite-difference large-eddy simulations,'' Phys. Fluids **7**, 2831 (1995).
[10] J. Smagorinsky, ''General circulation experiments with primitive equations,'' Mon. Weather Rev. **91**, 99 (1963).
[11] R. H. Kraichnan, ''Eddy viscosity in two and three dimension,'' J. Atmos. Sci. **33**, 1521 (1976).
[12] D. C. Leslie and G. L. Quarini, ''The application of turbulence theory to the formulation of subgrid modeling procedures,'' J. Fluid Mech. **91**, 65 (1979).
[13] C. E. Leith, ''Stochastic backscatter in a subgrid-scale model: Plane shear mixing layer,'' Phys. Fluids A **2**, 297 (1990).
[14] J. P. Chollet and M. Lesieur, ''Parametrization of small scales of three-dimensional isotropic turbulence utilizing spectral closures,'' J. Atmos. Sci. **38**, 2747 (1981).
[15] J. P. Bertoglio and J. Mathieu, ''A stochastic subgrid model for large eddy simulation: general formulation,'' C. R. Acad. Sci., Ser. II: Mec. Phys., Chim., Sci. Terre Univers **299**, 751 (1984).
[16] U. Schumann, ''Subgrid scales model for finite difference simulation of turbulent flows in plane channels and annuli,'' J. Comput. Phys. **18**, 367 (1975).
[17] P. Sullivan, J. C. McWilliams, and C. H. Moeng, ''A subgrid-scale model for large-eddy simulation of planetary boundary-layer flows,'' Boundary-Layer Meteorol. **71**, 247 (1994).
[18] J. A. Domaradzki and W. Liu, ''Energy transfer in numerically simulated wall-bounded turbulent flow,'' Phys. Fluids **6**, 1583 (1994).
[19] J. O'Neil and C. Meneveau, ''Subgrid-scale stresses and their modelling in a turbulent plane wake,'' J. Fluid Mech. **349**, 253 (1997).
[20] J. L. Lumley, ''Computational modeling of turbulent flows,'' Adv. Appl. Mech. **18**, 123 (1978).
[21] C. Pantano and S. Sarkar, ''DNS of mixing in compressible turbulent shear layers,'' Bull. Am. Phys. Soc. **42**, 2211 (1997).

[22]R. A. Clark, J. H. Ferziger, and W. C. Reynolds, ''Evaluation of subgrid-scale models using an accurately simulated turbulent flow,'' J. Fluid Mech. **91**, 1 (1979).
[23]C. Haertel, L. Kleiser, F. Unger, and R. Friedrich, ''Subgrid-scale energy transfer in the near-wall region of turbulent flows,'' Phys. Fluids **6**, 3130 (1994).
[24]J. H. Bell and R. D. Mehta, ''Development of a two-stream mixing layer from tripped and untripped boundary layers,'' AIAA J. **28**, 2034 (1990).
[25]A. W. Cook, ''Determination of the constant coefficient in scale-similarity models of turbulence,'' Phys. Fluids **9**, 1485 (1997).
[26]B. Vreman, B. Geurts, and H. Kuerten, ''Large-eddy simulation of the turbulent mixing layer,'' J. Fluid Mech. **339**, 357 (1997).
[27]U. Piomelli and Y Yu, ''Subgrid-scale energy transfer and near-wall turbulence structure,'' Phys. Fluids **8**, 215 (1996).
[28]S. Liu, J. Katz, and C. Meneveau, ''Evolution and modeling of subgrid scales during rapid straining of turbulence,'' J. Fluid Mech. (submitted).